REMARKS/ARGUMENTS

I. Status of the Claims

Claims 1-11, 52-58, and 68-78 are pending. Claims 12-18 and 25-52 have been canceled. Claims 59-67 and 79-103 have been withdrawn from examination.

II. The Amendments Herein

The amendments herein add no new matter.

The amendments to the specification add information about patent requested by the Examiner. One typographical error noted in one of the paragraphs being amended has also been corrected.

The amendments to claims 1 and 52 add a recitation that the binding specificity of the antibody is to the CD4-binding site of gp120. The recitation is supported throughout the specification, including page 12, lines 25-32. A recitation has also been added to claims 1 and 52 to clarify that the binding affinity is to gp120, as helpfully suggested by the Examiner. Support for the amendment is found throughout the specification, including page 32, lines 8-17 and Table 1. The amendment to claim 57 clarifies the claim, as helpfully suggested by the Examiner.

III. The Office Action

The Office Action rejects the claims on various grounds. Applicants amend in part and traverse the rejections. For the Examiner's convenience, the rejections are addressed below in the order in which they are presented in the Action.

A. Objections to the Specification

1. Objection that there is no abstract.

The Action objects to the specification as not containing an abstract and requires submission of an abstract on a separate sheet. Action at page 3. Applicants traverse.

Applicants respectfully observe that the application does in fact contain the required abstract. As in all published PCT applications, the abstract is printed on the face page of the application, at item (57), directly under the title. It therefore appears that the Action's objection is grounded on an inadvertent failure to note presence of the abstract. Reconsideration and withdrawal of the objection is respectfully requested.

For the sake of good order, Applicants also note that the abstract published in the PCT application meets U.S. filing requirements. Abstracts in PCT applications are filed by the applicants on a separate sheet following the claims (see, MPEP §1826, page 1800-39, left column), but the international authorities then print them on the first page. The published PCT applications are uniformly accepted by the PTO as meeting the requirements of U.S. national stage applications. The Action articulates no reason why this procedure, which is uniformly applied, would suddenly fail to be acceptable with respect to the present abstract.

2. References to U.S. Patents

The Action requires that the specification be updated to refer to U.S. Patents that have issued on referenced applications. Action at page 3.

The requested updates have been made. Applicants also noted a reference to a European application. Since it could not be immediately determined if the application had issued, and since the citation was part of a string of other citations making the same point, the reference to the European application was deleted.

3. References to SEQ ID NO:1

The Action indicates that SEQ ID NO:1 is the sequence of both the intact 3B3 antibody and 3B3(Fv). Action at page 3.

The specification has been amended to clarify the references to SEQ ID NO:1.

B. Rejections under 35 U.S.C. § 112

1. Rejection for alleged lack of enablement

Claims 8, 10, 55-56, 58, 74, 76, and 78 are rejected under 35 U.S.C. § 112, first paragraph, as allegedly not enabled. According to the Action: "[i]t is apparent that antibodies 3b3(Fv) and 3B3(dsFv) as well as immunotoxins 3B3(Fv)-PE38 and 3B3(dsFv)-PE38 are required to practice the invention. . . . Since the specification provides no sequences for said material and one of skill would not be able to discern what V_H and V_L sequences of the 3B3 antibody are incorporated into the claimed 3B3(Fv) or 3B3(dsFv), deposit of the aforementioned biological material is required." Action, at page 4. Applicants traverse.

The specification in fact sets forth not only the amino acid sequences for the V_H and V_L of 3B3(Fv), with an exemplar linker peptide, but also a nucleic acid sequence encoding the V_H, the V_L, and the linker. See, SEQ ID NOS:1 and 2. Thus, contrary to the Action's statements, the specification clearly sets forth "what V_H and V_L sequences of the 3B3 antibody are incorporated into the claimed 3B3(Fv)."

To the extent the Action's concerns go to the discussion of the cytotoxin PE38 or the creation of dsFv forms of the antibody, Applicants respectfully remind the Examiner that "[the test of enablement is whether one reasonably skilled in the art could make or use the invention from the disclosures in the patent coupled with information known in the art without undue experimentation.". MPEP § 2164.01, *quoting, United States v. Telectronics, Inc.*,857 F.2d 778, 785, 8 USPQ2d 1217, 1223 (Fed. Cir. 1988). Further, the MPEP §2164.01 reminds the Examining Corps that "[a] patent need not teach, and preferably omits, what is well known in the art. *In re Buchner*, 929 F.2d 660, 661, 18 USPQ2d 1331, 1332 (Fed. Cir. 1991); *Hybritech, Inc. v. Monoclonal Antibodies, Inc.*, 802 F.2d 1367, 1384, 231 USPQ 81, 94 (Fed. Cir. 1986), cert. denied, 480 U.S. 947 (1987)" (Emphasis added.)

Thus, under the standards articulated by the Courts, and imposed on the Examining Corps by the MPEP, enablement depends on whether one of skill could make or use the invention in light of not only the specification, but also information known in the art at the time of filing. With respect to the sequence of PE38, Applicants note that the specification states that PE38 "is a truncated *Pseudomonas* exotoxin composed of amino acids 253-364 and 381-

608." Specification, at page 18, lines 10-11. Thus, to make PE38, the person of skill needs only to know the sequence of native *Pseudomonas* exotoxin ("PE"). That sequence has been known in the art for years, as exemplified by SEQ ID NO:1 of U.S. Patent No. 5,602,095 (the '095 patent issued from the continuation of application 07/901,709, referenced in the current specification at page 18). The '095 patent issued in 1997, more than a year before the priority date of the present specification, and therefore was clearly available in the art to be coupled with the information in the present specification. (A copy of the '095 patent is enclosed herewith for the Examiner's convenience.) The formation of PE38 and of immunotoxins incorporating it was also specifically available in the art before the priority date of the present application. See, e.g., U.S. Patent No. 5,608,039, which also issued in 1997, at column 26, lines 5-12. (A copy of the '039 patent is enclosed herewith for the Examiner's convenience. To avoid confusion, Applicants note that the "B3" antibody discussed in the '039 patent is a murine antibody that binds to the "Lewis^{Y}" antigen present on some human cancers; it is not the same as the similarly named "3B3" antibody of the present invention, which binds to the glycoprotein gp120 of HIV-1)

With respect to the formation of disulfide-stabilized ("ds") Fvs, Dr. Pastan and his colleagues taught practitioners how to generate dsFvs from antibodies by mutating particular residues to cysteines in U.S. Patent No. 5,747,654, which issued in May 1997, again before the priority date of the present application. See, e.g., claim 2. The Examiner is respectfully reminded that a patent is presumed enabling for that which it claims. (A copy of the '654 patent is enclosed herewith for the Examiner's convenience.)

In addition to these teachings available in the art, the application also sets forth methods known in the art for expressing the nucleic acid (e.g., specification, at page 22, lines 15-21), methods for chemical conjunction of the antibody to a effector molecule (e.g., page 20, line 18, to page 22, line 7), and methods for expressing the antibody-cytotoxin construct as a fusion protein (e.g., specification at page 22, line 8 to page 25, line 19). Moreover, the specification contains a working example describing for the person of skill how such constructs were actually made. See, specification at page 31, line 16, to page 32, line 3.

Thus, Applicants respectfully maintain that, in the words of the Court cited by MPEP 2164.01, "one reasonably skilled in the art could make or use the invention from the disclosures in the patent coupled with information known in the art without undue experimentation." The application sets forth the sequence information sufficient to permit the practitioner to make and use the invention in combination with information known in the art. Thus, deposit of the materials discussed in the Action is not necessary to enable the invention. Reconsideration and withdrawal of the rejection is respectfully requested.

2. Rejection under 35 U.S.C. § 112, second paragraph

Claims 1-11 and 52-58 are rejected under 35 U.S.C. § 112, second paragraph, as allegedly indefinite for use of the phrase "a minimum binding affinity of 3B3." According to the Action, it is unclear if this phrase refers to the binding to gp120 or to some other antigen. Action, at page 5. Claims 1 and 52 have been amended to recite that the binding affinity and specificity of 3B3 are with respect to gp120.

3. Rejection of claim 57

Claim 57 is rejected as allegedly vague and indefinite by the term "FV("dsFv"). Action, at page 5. The claim has been amended to increase its clarity.

C. Rejections of the Claims as Anticipated

1. Rejection over Bera et al.

Claims 1-11, 52-56, 68-74, 77, and 78, are rejected under 35 U.S.C. § 102(a) as anticipated by Bera et al., Mol. Med. 4:384-391 (1998) ("Bera"). The Action notes that the availability of the Bera reference was being determined and that the rejection would be withdrawn if the reference was not publicly available before the priority date.

The Bera reference was not available before the June 11, 1998 priority date of the present application. Applicants' counsel had occasion to answer this question in 2002 in connection with one of the foreign equivalents of the present application. Attached is a copy of email correspondence from 2002 between the undersigned counsel for the Applicants and Dr.

Yvonne Cole, then the editor of the journal "Molecule Medicine." Dr. Cole indicated in her email that the mail date for the issue in question was June 30, 1998.

Accordingly, the Bera reference was not available to the public as of the priority date of the application and is not available as a reference under §102(a). The rejection should be reconsidered and withdrawn.

For the sake of good order, Applicants also point out that, in any event, the Bera reference would not be available as a reference for purposes of §102(a). Section 102(a) requires on its face that the invention "be known or used by others . . . before the invention thereof by the applicant for patent." (Emphasis added). Thus, at a minimum, for a reference to be applied under §102(A), it must constitute the work of another. Applicants respectfully note that the inventors of the present application are:

Ira H. Pastan, Tapan K. Bera, Paul E. Kennedy, Edward A. Berger, and Carlos F. Barbas, III.

The authors of the Bera reference are listed as:

Tapan K. Bera, Paul E. Kennedy, Edward A. Berger, Carlos F. Barbas III, and Ira Pastan. Thus, there is no difference between the authors of the Bera reference and the inventors of the present application. The Bera reference is therefore not evidence that the invention that the invention was "known or used by others," as required for a reference under §102(a). For this separate reason as well, the rejection should be reconsidered and withdrawn.

2. Rejection over Matsushita et al.

Claims 1-3, 6, 11, 57, 68, 69, 72, and 75 are rejected under 35 U.S.C. § 102(b) as anticipated by Matsushita et al., AIDS Research and Human Retroviruses, 6:193-203 (1990) ("Matsushita"). According to the Action, Matsushita discloses an anti-gp120 immunotoxin of the 0.5β antibody coupled to PE. The Action indicates that, in the absence of evidence to the contrary, the 0.5β antibody is deemed to inherently have a binding affinity equal to or greater than the 3B3 antibody. Action, at page 8. Applicants amend in part and traverse.

Claims 1 and 52 have been amended to recite that the claimed immunotoxins bind the CD4-binding site of gp120. It was known before the priority date of the invention that the

0.5β antibody binds a determinant "within a disulfide-bridged loop in the third hypervariable region (V3) of gp120." Faiman et al., J Biol Chem 271(23):13829-13833 (1996), at page 13829, left column. (A copy of Faiman et al. 1996 is enclosed for the Examiner's convenience.) The V3 loop that is bound by the 0.5β antibody is not the same section of gp120 as the CD4-binding site. Attached for the Examiner's convenience is a copy of Wyatt et al., Nature, 393:705-709 (1998). Figure 2 of Wyatt et al., on page 708, shows the spatial relationship of epitopes on the HIV-1 gp120 glycoprotein. As shown in Figure 2a, the upper left hand figure, the V3 loop bound by the 0.5β antibody is located on the lower right hand side of gp120, as it is modeled in this Figure. By contrast, as shown in Figures 2b and 2c, the CD4 binding site is located in a cleft on the middle left hand side of the gp120 molecule (the abbreviation "CD4BS" is defined as referring to the CD4-binding site on page 706, left column, second full paragraph).

Thus, the claims as amended recite an antibody that has a different binding specificity than that of the 0.5β antibody. As stated in MPEP § 2131.01, "[a] claim is anticipated only if each and every element as set forth in the claim is found, either expressly or inherently described, in a single prior art reference." *Verdegaal Bros. v. Union Oil Co. of California*, 814 F.2d 628, 631, 2 USPQ2d 1051, 1053 (Fed. Cir. 1987). Since the 0.5β antibody does not bind the CD4-binding site of gp120, as now recited in claims 1 and 52, the Matsushita reference does not contain every element of the claims, as required for a proper anticipatory reference under §102(b). Accordingly, the rejection should be reconsidered and, upon reconsideration, withdrawn.

D. Rejection of the Claims as Obvious

1. Rejection of the Claims over Bera

Claims 57, 58, 75, and 76 have been rejected under 35 U.S.C. § 103(a) as obvious over Bera, *supra.* Action, at page 9. The Action notes that the rejection would be withdrawn if Bera was determined not to be publicly available before the priority date.

As set forth in Section C 1, above, the Bera reference was not available to the public as of the priority date of the application. It therefore is not available as a reference under

§103(a). The rejection of the claims as obvious over the reference should therefore be reconsidered and withdrawn.

2. Rejection of the Claims as Obvious over Matsushita

Claims 1-6, 8, 9, 11, 52-55, 57, 68-72, and 74-77 are rejected under 35 U.S.C. § 103(A) as obvious over Matsushita, supra. According to the Action, Matsushita et al. discloses the anti-gp120 antibody 0.5β coupled to PE. The Action states that, given that Matsushita discloses an antibody reactive with a number of HIV isolates, it would have been obvious for one of ordinary skill to use the 3B3 antibody in the Matsushita immunotoxin. Applicants traverse.

The rejection rests on the assumption that the person of skill in the art would have been motivated to modify the Matsushita antibody based on the results set forth in the reference. But, Matsushita was published in 1990. Following the publication of Matsushita, the only anti-HIV-1 immunotoxin to reach clinical trials (the immunotoxin was also directed against HIV-1 env) showed disappointing results. As reported by Ramachandran et al., J. Infect Dis 170:1009-13 (1994), patient HIV-1 proviral levels remained the same before and after immunotoxin treatment. Similarly, Davey et al., J. Infect Dis 170:1180-8 (1994) reported no consistent changes in immunologic or virologic markers in patients to whom anti-HIV-1 immunotoxin was administered. (For the Examiner's convenience, copies of the Medline abstracts of these publications are enclosed.) Moreover, an immunotoxin using a portion of the CD4 molecule containing the gp120 binding site had unexpectedly high toxicity. See, specification, at page 35, line 26 to page 36, line 6. In the wake of these reports, the approach of using anti-HIV antibodies as targeting moieties for anti-HIV immunotoxins was abandoned. See, e.g., Goldstein et al., J. Infect Dis 181:921-926 (2000), at page 921, right column, bottom paragraph (for the Examiner's convenience, a copy of Goldstein is enclosed). Therefore, the teachings in the art shortly after the publication of Matsushita were that use of anti-gp120 antibodies to target immunotoxins to HIV-infected cells would not work.

As the Examiner will recall, obviousness is measured by what would have been obvious at the time the invention was made. The person of skill in the art at the time the invention was made would have been aware not just of Matsushita, but also the fact that

immunotoxins to kill HIV-infected cells had failed in clinical trial. Accordingly, following the 1994 publication of the results of the clinical trials of the first anti-HIV-1 immunotoxin, no motivation existed in the art to create immunotoxins targeted by anti-HIV-1 antibodies against HIV-1.

Accordingly, even assuming that the Action's citation of Matsushita gave rise to a *prima facie* case of obviousness, that *prima facie* case was destroyed by developments in the art after the date of Matsushita's publication. Reconsideration of the rejection, and its withdrawal, are respectfully requested.

CONCLUSION

In view of the foregoing, Applicants believe all claims now pending in this Application are in condition for allowance. The issuance of a formal Notice of Allowance at an early date is respectfully requested.

If the Examiner believes a telephone conference would expedite prosecution of this application, he is invited to telephone the undersigned at 415-576-0200.

Respectfully submitted,

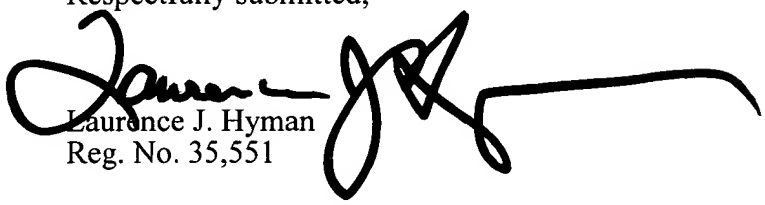

Laurence J. Hyman
Reg. No. 35,551

TOWNSEND and TOWNSEND and CREW LLP
Two Embarcadero Center, Eighth Floor
San Francisco, California 94111-3834
Tel: 415-576-0200
Fax: 415-576-0300
Attachments
LJH:ljh
60079712 v1

Attachments: Emails to and from editor of Mol. Med.
U.S. Patent Nos. 5,602,905, 5,608,039, and 5,747,654
Ramachandran abstract
Davey abstract
Goldstein article
Faiman 1996
Wyatt 1998

From: "Yvonne Cole" <ycole@picower.edu>
T : "Laurence J. Hyman" <ljhyman@townsend.com>
Date: Wednesday, January 16, 2002 2:04PM
Subject: Re: Publication date

Dear Mr. Hyman:
I am very sorry for the confusion. I realised after our last communication that Springer-Verlag was the publisher of note. I have contacted the production manager at Springer-Verlag, and the compositor/printer (Cadmus) as well. Both agree, the mail date was June 30, 2002, and the issue did not appear online or on display at any time prior to that date.
Best regards,

********** REPLY SEPARATOR **********

On 1/16/02 at 12:41 PM Laurence J. Hyman wrote:

>Dear Dr Cole:
>Mr Breichner has informed me that JHU was not the publisher of Mol Med in >1998, and that he therefore could not provide the mail date for the June >1998 issue in question. He thought your publisher at that time might have >been Springer Verlag. Would you be able to provide me with the name of a >person at Springer Verlag I might be able to contact to get the mail date >information? Thanks so much.
> Regards,
> Larry Hyman
>
>Laurence J. Hyman
>TOWNSEND AND TOWNSEND AND CREW, LLP
>2 Embarcadero Center, 8th Flr.
>San Francisco, CA 94111
>(P) 415/576-0200
>(F) 415/576-0300
>ljh@townsend.com

>
>>>> "Yvonne Cole" <ycole@picower.edu> 1/7/02 2:27:43 PM >>>
>Dear Mr. Hyman:
>Thank you for your email. I have forwarded your request to our publisher >(The Johns Hopkins University Press), who can supply the information you >need. If you don't hear from them in due time, please contact the Journals >Director and Production Manager, Bill Breichner,
>wbreichner@mail.press.jhu.edu.

>Best regards,
>
>
>
>********** REPLY SEPARATOR **********
>
>On 1/7/02 at 1:38 PM Laurence J. Hyman wrote:
>
>>Dear Dr. Cole:
>> Dr. Ira Pastan of the NIH gave me your name as the contact person for the
>>journal "Molecular Medicine." In 1998, Dr. Pastan and his colleagues
>>published an article in your journal: Bera et al., Mol Med 4:384-91 (June
>>1998). It has now become important to determine the actual date the issue
>>containing this article was mailed from the publisher (and, if the article
>>was placed on line before the mail date of the issue, the date that it was
>>actually placed on line). It would be greatly appreciated if you or the
>>appropriate person on your staff could provide this information.
>> I am the NIH's counsel with respect to this matter. If you have any
>>questions, please feel free to contact me by replying to this email, by
>>phone (direct line: 415/273-4744) or by fax (415/576-0300).
>> Very truly yours,
>> Laurence J. Hyman
>> Townsend and Townsend and Crew, LLP
>> 2 Embarcadero Center
>> San Francisco, CA 94109
>>
>>cc: Dr. Ira Pastan
>
>
>Yvonne I Cole, Ph.D.
>Managing Editor
>Molecular Medicine
>The Picower Institute for Medical Research
>350 Community Drive (4th Floor)
>Manhasset, New York 11030
>Tel: 516-562-9415
>Fax: 516-869-8428
>email: ycole@picower.edu

Yvonne I Cole, Ph.D.
Managing Editor
Molecular Medicine
The Picower Institute for Medical Research
350 Community Drive (4th Floor)
Manhasset, New York 11030
Tel: 516-562-9415
Fax: 516-869-8428
email: ycole@picower.edu

MEDLINE

- Search

Browse by Journal

Browse MESH

Preferences

About MEDLINE

Quick Site Search

GO

BioMedNet

Advanced site search

Medline

Simple | Advanced | Citation | History | Results | Record

Reconsidering targeted toxins to eliminate HIV infection: you gotta have HAART.

Berger EA, Moss B, Pastan I

Proc Natl Acad Sci U S A 1998 Sep 95:11511-3

BROWSE : Proc Natl Acad Sci U S A • Volume 95 • Issue 20

VIEW : **MEDLINE**, full MEDLINE, related records, full text

Abstract

The success of highly active anti-retroviral therapy (HAART) has inspired new concepts for eliminating HIV from infected individuals. A major obstacle is the persistence of long-lived reservoirs of latently infected cells that might become activated at some time after cessation of therapy. We propose that, in the context of treatment strategies to deliberately activate and eliminate these reservoirs, hybrid toxins targeted to kill HIV-infected cells be reconsidered in combination with HAART. Such combinations might also prove valuable in protocols aimed at preventing mother-to-child transmission and establishment of infection immediately after exposure to HIV. We suggest experimental approaches in vitro and in animal models to test various issues related to safety and efficacy of this concept.

MeSH

Animal; Anti-HIV Agents; Clinical Trials, Phase I; Disease Transmission, Vertical; Exotoxins; Female; Gene Products, env; HIV; HIV Infections; Human; Immunotoxins; Liver; Models, Biological; Pregnancy; Proviruses; Recombinant Proteins; Support, U.S. Gov't, P.H.S.; Toxins; Virus Activation

Comments

Erratum in: Proc Natl Acad Sci U S A 1999 Feb 2;96(3):1162

Author Address

Laboratory of Viral Diseases, National Institute of Allergy and Infectious Diseases, National Institutes of Health, Bethesda, MD 20892, USA. edwardvberger@nih.gov

Medline

Failure of short-term CD4-PE40 infusions to reduce virus load in human immunodeficiency virus-infected persons.

Ramachandran RV, Katzenstein DA, Wood R, Batts DH, Merigan TC

J Infect Dis 1994 Oct 170:1009-13

BROWSE : J Infect Dis • Volume 170 • Issue 4

VIEW : **MEDLINE**, full MEDLINE, related records

Abstract

The safety, immunologic, and antiviral effects of a recombinant biologic product that combines the second and third domains of the CD4 molecule and Pseudomonas exotoxin A (PE40) were evaluated in 21 human immunodeficiency virus (HIV)-infected subjects in a phase III open-label dose-ranging study. Subjects with CD4+ lymphocyte counts of 100-500/mm3 received CD4-PE40 at 40, 80, or 160 micrograms/m2 by infusion three to seven times over 10 days. At the maximum tolerated dose (80 micrograms/m2), peak CD4-PE40 levels were 65-130 ng/mL with a serum half-life of 3.6 +/- 1.5 h. Toxicity, primarily increased hepatic transaminases, was dose-related and reversible. HIV DNA proviral levels in peripheral blood mononuclear cells and plasma HIV RNA remained stable during and after CD4-PE40 infusions. The relative resistance of clinical isolates of HIV, limits of the tolerated dose, and the immunogenicity and short half-life of the protein may explain the lack of in vivo antiviral effect of CD4-PE40.

MeSH

Adult; Antigens, CD4; CD4-Positive T-Lymphocytes; DNA, Viral; Drug Administration Schedule; Exotoxins; HIV; HIV Seropositivity; Human; Immunotoxins; Infusions, Intravenous; Proviruses; Pseudomonas aeruginosa; RNA, Viral; Support, Non-U.S. Gov't; Treatment Failure

Author Address

Center for AIDS Research, Stanford University Medical Center, California 94305.

Medline

Use of recombinant soluble CD4 Pseudomonas exotoxin, a novel immunotoxin, for treatment of persons infected with human immunodeficiency virus.

Davey RT, Boenning CM, Herpin BR, Batts DH, Metcalf JA, Wathen L, Cox SR, Polis MA, Kovacs JA, Falloon J

J Infect Dis 1994 Nov 170:1180-8

BROWSE : J Infect Dis • Volume 170 • Issue 5

VIEW : **MEDLINE**, full MEDLINE, related records

Abstract

Single and multiple doses of sCD4-PE40, a soluble recombinant fusion toxin selectively toxic to gp120-expressing cells, were evaluated in persons infected with human immunodeficiency virus type 1 (HIV-1). Seventeen of 24 patients who completed a single-dose safety trial were given either 1, 5, 10, or 15 micrograms/kg of sCD4-PE40 by intravenous bolus once a month for 2 months, then weekly for 6 weeks. The weekly maximally tolerated dose was 10 micrograms/kg. The major toxicity was a transient dose-dependent elevation in hepatic aminotransferases peaking 48 h after infusion. Anti-Pseudomonas exotoxin antibody developed in 58% of recipients, and sera from 13 of 17 showed neutralizing activity against sCD4-PE40. No consistent changes in immunologic or virologic markers were observed. Weekly infusions of < or = 10 micrograms/kg of sCD4-PE40 are generally well tolerated, but additional studies correlating optimal dosing and frequency of administration with efficacy will be needed to define the role of this novel agent in the management of HIV-1-infected patients.

MeSH

Adolescence; Adult; Antigens, CD4; Antiviral Agents; Exotoxins; HIV Infections; Human; Immunotoxins; Middle Age; Recombinant Proteins; Single-Blind Method; Support, Non-U.S. Gov't; Support, U.S. Gov't, P.H.S.

Author Address

National Institute of Allergy and Infectious Diseases, National Institutes of Health, Bethesda, Maryland 20892.

Chimeric Toxins Targeted to the Human Immunodeficiency Virus Type 1 Envelope Glycoprotein Augment the In Vivo Activity of Combination Antiretroviral Therapy in thy/liv-SCID-Hu Mice

Harris Goldstein,[1,2] Massimo Pettoello-Mantovani,[2] Tapan K. Bera,[3] Ira H. Pastan,[3] and Edward A. Berger[4]

Departments of [1]Pediatrics and of [2]Microbiology and Immunology, Albert Einstein College of Medicine, Bronx, New York; [3]Laboratory of Molecular Biology, National Cancer Institute, and [4]Laboratory of Viral Diseases, National Institute of Allergy and Infectious Diseases, National Institutes of Health, Bethesda, Maryland

Highly active antiretroviral therapy (HAART), which combines multiple inhibitors of essential human immunodeficiency virus type 1 (HIV-1) enzymes, induces dramatic and sustained viral load reductions in many people infected with HIV-1. However, reservoirs of infected cells capable of producing replication-competent virus persist even after years of HAART, preventing elimination of infection. CD4-PE40 and 3B3(Fv)-PE38, chimeric toxins designed to target the HIV envelope (Env), represent a complementary class of agents that selectively kill productively infected cells. To investigate whether these Env-targeted toxins might serve as adjuncts to HAART for the elimination of infected cells, we tested their ability to augment HAART efficacy in vivo by using a thy/liv SCID-hu mouse model. CD4-PE40 and 3B3(Fv)-PE38 markedly enhanced the capacity of HAART to suppress acute HIV-1 infection and improved HAART-mediated viral load reduction in mice with established HIV-1 infection. These results represent the first demonstration of in vivo anti–HIV-1 efficacy for Env-targeted toxins and support their potential therapeutic utility in combination with HAART.

Highly active antiretroviral therapy (HAART), which combines multiple inhibitors of essential enzymes of human immunodeficiency virus type 1 (HIV-1), promotes dramatic and sustained viral load reductions in plasma and tissues of many HIV-1–infected persons [1]. The associated clinical improvements and reduced death rates have transformed perspectives on HIV-1 treatment. However, it has become clear that HAART does not eradicate HIV-1 infection from the body. Reservoirs of cells harboring replication-competent virus persist in blood, lymphoid tissue, and the male genital tract even after years of treatment [2–7]; moreover, low level HIV-1 replication continues in the face of suppressive HAART [4, 8–16]. These persistent virus sources are presumed to make major contributions to the rapid HIV-1 rebound observed after cessation of therapy [17–20] and are therefore considered the major barriers to eliminating infection.

Hybrid protein toxins designed to target the HIV Env glycoprotein on the surface of productively infected cells are a complementary class of anti-HIV agents [21]. Their potent activities result not from blocking of virus replication, but from selective killing of infected cells. Such proteins contain an Env-binding moiety such as CD4 or an anti-Env antibody, linked to the effector domains of a protein toxin such as *Pseudomonas* exotoxin A (PE), ricin, or diphtheria toxin. To date, only 1 Env-targeted toxin has been tested in human clinical trials: a recombinant protein designated CD4-PE40 that contains a region of CD4 linked to the translocation and cytotoxic moieties of PE [22]. Early studies in vitro indicated highly desirable anti-HIV-1 properties, alone and in combination with reverse transcriptase inhibitors (see [23] for original citations). However, disappointing results from phase I trials conducted in the pre-HAART era [24, 25] caused this approach to be abandoned. With the subsequent development of HAART and the awareness of the need to eliminate the long-lived infected cell res-

Received 8 September 1999; revised 8 December 1999; electronically published 20 March 2000.

Presented in part: The Keystone Symposium on AIDS Pathogenesis, January 1999, Keystone, CO.

Informed consent was obtained from patients. This study followed the human experimentation guidelines of the US Departments of Health and Human Services and the Albert Einstein College of Medicine in the conduct of clinical research and followed the animal experimentation guidelines of the Albert Einstein College of Medicine in animal studies.

Financial support: National Institutes of Health (NIH; National Institute of Neurological Disorders and Stroke NS39201 and Centers for AIDS Research Grant AI-27741) and by the NIH Intramural AIDS Targeted Antiviral Program. M.P.M. was supported by an NIH training grant (CA09173).

Some of the authors of the manuscript either have patents or patents pending on the Env-targeted toxins described in the paper. E.A.B. is an inventor on US-owned patents related to CD4-PE40 and on US patent application for 3B3(Fv)-PE38. I.P. is an inventor on patents related to PE technology, on US-owned patents related to CD4-PE40, and on US patent application for 3B3(Fv)-PE38. T.B. is an inventor on US patent application for 3B3(Fv)-PE38. We do not feel that their patent position poses a conflict of interest for the findings presented in this paper.

Reprints or correspondence: Dr. Harris Goldstein, Albert Einstein College of Medicine, Chanin Bldg., Rm. 601, 1300 Morris Park Ave., Bronx, NY 10461 (hgoldste@aecom.yu.edu).

The Journal of Infectious Diseases 2000; 181:921–6

0022-1899/2000/18103-0015$02.00

ervoirs, we recently proposed that the specific cytotoxic activity of Env-targeted toxins against HIV-1–infected cells warrants renewed consideration [23]. We suggested various experimental approaches, both in vitro and in vivo, to test the efficacy and safety of these agents when used in conjunction with HAART. Presently there are no published data showing the in vivo efficacy of Env-target toxins, either alone or in combination with other antiretrovirals.

In the present study, we evaluated the capacity of Env-target toxins to enhance HAART efficacy in vivo in a mouse model. We used SCID mice implanted with human fetal thymus and liver tissue under the kidney capsule (thy/liv-SCID-hu mice). We have previously shown that this model is well suited for evaluating the efficacy of different regimens of HAART in vivo, in both prevention and treatment modes [26]. Two distinct chimeric toxins were tested: CD4-PE40 and 3B3(Fv)-PE38 [27], which is a potent immunotoxin containing the effector portions of PE linked to a single-chain Fv from an affinity-enhanced, broadly cross-reactive antibody against the CD4-binding region of gp120. Our results reveal the ability of Env-targeted toxins to significantly enhance the anti-HIV-1 activity of HAART in experimental protocols examining both the prevention of acute infection and the treatment of chronic infection.

Materials and Methods

Env-targeted toxins and control proteins. CD4-PE40 and sCD4 (first 2 extracellular domains, amino acids 1–183) were donated by Shirley Johnson at Pharmacia-Upjohn, Kalamazoo, MI. The control immunotoxin, RFB4(dsFv)-PE38, is directed at the human B cell antigen CD22 [28] and is not expected to affect HIV-1 infection. We generated sCD4 using mammalian cell expression, and the chimeric toxins were produced using bacterial expression [22, 27].

Implantation of human thymic and liver tissue into SCID mice. The thy/liv-SCID-hu mice were constructed by implanting human fetal thymic and liver tissue obtained from 17–21-gestational-week fetuses within 8 h after the elective termination of pregnancy into SCID mice (6–8 weeks old) as described elsewhere [26]. Briefly, about 10 pieces of syngeneic human fetal thymic and liver tissue were implanted under the left and right kidney capsules of SCID mice anesthetized with pentobarbital (40–80 mg/kg). The procedure was associated with minimal morbidity and mortality and was successful in >95% of the mice, as indicated by a >20-fold increase in size of the implanted tissue 3 months later. We used flow cytometry to confirm the population of human T cells and monocytes in the peripheral blood of these mice; in the mice used for these experiments, the peripheral blood contained >5% human leukocytes. The consent forms and procedures used in this study were reviewed and approved by the Albert Einstein College of Medicine Committee on Clinical Investigation.

Infection of thy/liv-SCID-hu mice with HIV. HIV-1_{59}, an R5 (CCR5-specific, nonsyncytium-inducing) primary isolate, was derived from peripheral blood mononuclear cells (PBMC) by coculture with phytohemagglutinin (PHA)-activated donor PBMC [29] from a 17-month-old child infected with HIV-1; the virus was expanded by another round of coculture with PHA-activated PBMC and then divided into aliquots that were frozen in liquid nitrogen [26, 29]. thy/liv-SCID-hu mice were infected by intraperitoneal (ip) injection of 8000 $TCID_{50}$ of the HIV-1_{59} in a volume of 500 μL. To control for variability due to the source of donor tissue and degree of reconstitution with human cells, we ensured that each treatment group contained mice engrafted with the same donor tissue and with similar quantities of human cells in their peripheral blood.

Administration of HAART and Env-targeted toxins. We administered HAART to the mice by mixing the indicated drugs with powdered animal feed and then adding the mixture to feeding jars that were designed to minimize spillage. The drug dosage for each mouse was calculated on the basis of the average oral intake of 5 g of diet per day (each mouse weighed ~25 g). Mice were treated with HAART comprised of zidovudine (100 mg kg^{-1} day^{-1}), lamivudine (100 mg kg^{-1} day^{-1}), and ritonavir (200 mg kg^{-1} day^{-1}) or suboptimal HAART (10% of the dose for each HAART drug) as described elsewhere [26]. The thy/liv-SCID-hu mice were housed singly so that drug consumption could be confirmed by measurement of the quantity of feed consumed. The Env-targeted toxins were administered by ip injection of the indicated dose in PBS in 5 doses given on alternate days.

Titration of HIV-infected mononuclear cells in the hu-thy/liv implant by limiting dilution coculture. The level of HIV-1 infection in the hu-thy/liv implants was determined by measuring the number of HIV-1–infected thymocytes present in a wedge biopsy of the implant by quantitative coculture, as described elsewhere [26, 29]. Five-fold dilutions of mononuclear cells isolated from the hu-thy/liv implants (range, 1×10^6–3.2×10^2 cells) were cultured in quadruplicate at 37°C in 24-well culture plates with PHA-activated donor mononuclear cells (1×10^6) in 2 mL of RPMI 1640 containing fetal calf serum (10% v/v) and interleukin-2 (32 U/mL). The p24 antigen content of the culture supernatant was measured 1–2 weeks later by means of the HIV-1 p24 core profile ELISA assay (DuPont-NEN, Wilmington, DA). The number of HIV-1–infected thymocytes in the implants is reported as TCID/10^6 thymocytes, which was calculated by determining the lowest number of added thymocytes that infected at least half of the quadruplicate cultures with HIV-1. Productive infection after the addition of the lowest number of added thymocytes (320 cells) was scored as 3125 TCID/10^6 thymocytes.

Statistical analysis. Statistical significance of the data were evaluated by using the Student's t test.

Results

Env-targeted toxins enhance capacity of HAART to suppress acute HIV-1 infection. We have shown previously that, whereas HAART that is initiated immediately after HIV-1 inoculation of thy/liv-SCID-hu mice prevents establishment of infection, suboptimal HAART (10-fold lower doses of the same drugs) strongly suppresses HIV-1 levels during the treatment period, but does not prevent the subsequent appearance of viral load at 1 month after the cessation of treatment [26]. Here, we examined the in vivo antiretroviral effect of Env-targeted toxins by determining whether they augmented the activity of suboptimal HAART. Thy/liv-SCID-hu mice were infected by ip in-

oculation of HIV-1_{59} [29], then immediately started on the indicated treatment. After 1 month, the effects of the different treatments on HIV-1 infection were determined by quantitating HIV-1–infected thymocytes in a biopsy of the hu-thy/liv implants; this method is much more sensitive than measuring plasma HIV RNA and can quantitate viral load in HAART-treated animals that have no detectable plasma viremia [26]. The mice were then taken off therapy, and 1 month later the hu-thy/liv implants were biopsied again and analyzed.

The effects on suboptimal HAART alone or Env-targeted toxins alone are shown in figure 1. In contrast to untreated mice, in which extensive infection (mean = 2708 TCID/10^6 thymocytes) was detected in the thy/liv implants at both 1 and 2 months after virus inoculation, mice maintained on suboptimal HAART did not have detectable HIV-1 infection at the end of the 1-month treatment period (mean = 0 TCID/10^6 thymocytes). However, HIV-1 infection emerged during the 1-month period after cessation of therapy (mean = 258 TCID/10^6 thymocytes), which is consistent with our previous findings with this suboptimal HAART regimen [26]. The Env-targeted toxins alone suppressed infection only modestly compared with HAART, but the antiretroviral effects were significant (for CD4-PE40, mean = 975 TCID/10^6 thymocytes, $P = .028$; for 3B3(Fv)-PE38, mean = 292 TCID/10^6 thymocytes, $P = .003$). In contrast, the mixture of sCD4 plus the control toxin RFB4(dsFv)-PE38 did not significantly suppress HIV infection in the thy/liv implants (mean = 1875 TCID/10^6 thymocytes, $P = .15$), which indicates that the effects seen with the Env-targeted toxins resulted from selective killing of infected cells.

We next examined whether Env-targeted toxins could enhance the efficacy of suboptimal HAART in suppressing acute HIV-1 infection in the thy/liv-SCID-hu mice. As shown in table 1, the viral loads in the hu-thy/liv implants at 1 month after cessation of therapy remained markedly suppressed in the mice treated with the combination of lower-dose HAART plus either Env-targeted toxin, in contrast to the mice treated with HAART alone, in which the viral load increased significantly. Again, the control proteins sCD4 plus RFB4(dsFv)-PE38 did not augment the anti-HIV-1 activity of HAART, which verified that the activities seen with the Env-targeted toxins reflected specific killing of infected cells, not simple neutralization by the CD4 moiety or nonspecific toxicity by the PE moiety. Thus, by virtue of their specific cytotoxic activities, the Env-targeted toxins administered immediately after HIV-1 inoculation greatly enhanced the capacity of suboptimal HAART to suppress acute infection.

Env-targeted toxins enhance the capacity of HAART to treat established HIV-1 infection. We have shown previously that HAART significantly decreases the level of infection in the hu-thy/liv implants of thy/liv SCID-hu mice with established HIV-1 infection, but does not eradicate it, as evidenced by the moderate numbers of residual HIV-1–infected cells that remain in the thymic implants [26]. Therefore, we also used the thy/liv-SCID-hu mouse system to examine the ability of Env-targeted toxins to augment HAART for treating established in vivo HIV-1 infection. One month after ip inoculation with HIV-1_{59}, the baseline level of HIV-1 infection was determined by quantitative coculture of biopsies from the hu-thy/liv implants; the values were 3125 $TCID_{50}/10^6$ thymocytes for each of the infected mice. The mice were then treated with HAART alone, HAART plus CD4-PE40, or HAART plus 3B3(Fv)-PE38. After 1 month of treatment, the effects of these therapeutic regimens on HIV infection in the treated mice were determined by quantitative coculture of repeat biopsies of the hu-thy/liv implants. In the untreated mice, the levels of infection in the implants did not decrease, remaining at 3125 $TCID_{50}/10^6$ thymocytes. By contrast, as shown in table 2, the viral loads in the thy/liv implant decreased significantly in the mice treated with HAART alone ($P < .001$), HAART plus CD4-PE40 ($P < .001$), or HAART plus 3B3(Fv)-PE38 ($P < .001$). With HAART plus 3B3(Fv)-PE38,

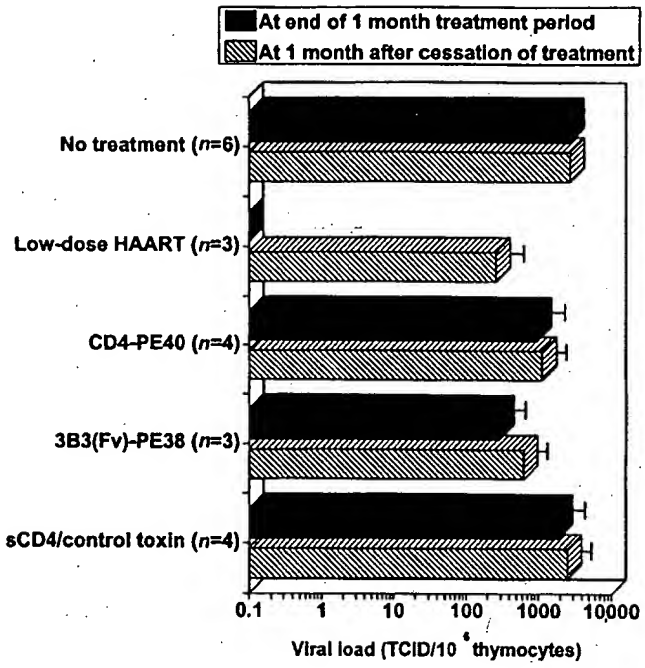

Figure 1. Effects of suboptimal highly active antiretroviral therapy (HAART) or human immunodeficiency virus (HIV) envelope-targeted toxins on acute HIV-1 infection in vivo. thy/liv-SCID-hu mice were injected intraperitoneally with HIV-1_{59} (8000 $TCID_{50}$). The mice were then left untreated or were immediately started either on suboptimal HAART, CD4-PE40, 3B3(Fv)-PE38, or a control mixture of sCD4 plus RFB4(dsFv)-PE38 (control toxin); toxins were administered at a total dose of 5 μg given in 5 equal doses on alternate days beginning at day one. One month later, the left thy/liv implants were biopsied, and viral loads were analyzed by quantitative coculture *(dark bars)*. Drug therapy was then stopped, and after 1 month the left thy/liv implant of each mouse was rebiopsied and the viral load quantitated *(light bars)*. The data are presented as the TCID/10^6 thymocytes, determined by limiting dilution coculture; the mean values (±SEM) were calculated for each treated group.

Table 1. Measurements of viral load in thy/liv-SCID-hu mice infected with acute human immunodeficiency virus (HIV), showing that HIV envelope-targeted toxins enhance the ability of suboptimal highly active antiretroviral therapy (HAART) to suppress acute HIV in vivo.

Treatment (dose), mouse no.	Viral load, TCID/10^6 thymocytes	
	At end of 1-mo treatment period	1 mo after end of treatment
None		
261-a3	3125	3125
261-a4	625	625
261-b2	3125	3125
253-b5	3125	3125
259-a2	3125	3125
250-a3	3125	3125
Mean ± SEM	2708 ± 416	2708 ± 416
Suboptimal HAART		
250-b2	0	25
250-b3	0	125
253-b4	0	625
Mean ± SEM	0	258 ± 185
Suboptimal HAART plus:		
CD4-PE40 (50 ng)		
252-a4	0	0
252-a3	0	0
252-b	0	0
Mean	0	0
CD4-PE40 (5 μg)		
261-a1	0	0
261-a5	1	5
265-a3	0	1
Mean ± SEM	0.3 ± 0.2	2 ± 1.5
3B3(Fv)-PE38 (50 ng)		
253-a3	0	0
253-a4	0	0
250-a5	0	0
Mean ± SEM	0	0
3B3(Fv)-PE38 (5 μg)		
261-c2	0	1
265-a4	0	1
Mean ± SEM	0	1 ± 0
sCD4 + control toxin (5 μg)[a]		
258-2	0	125
265-b5	0	125
265-d5	0	625
258-3	0	125
Mean ± SEM	0	250 ± 125

NOTE. The mice were injected intraperitoneally with HIV-1_{99} (8000 $TCID_{50}$) and either not treated or immediately started on treatment. Dose amounts are the total amount of drug administered in 5 equal doses on alternate days beginning at day 1.

[a] RFB4(dsFv)-PE38 (5 μg), a negative control toxin not expected to affect HIV infection. The data are presented as the TCID/10^6 thymocytes, determined by limiting dilution coculture.

the viral load was significantly lower ($P = .04$) than with HAART alone (mean, 10.3 ± 5.7 vs. 91.7 ± 26 TCID/10^6 thymocytes). This demonstrates that 3B3(Fv)-PE38 can augment the antiretroviral activity of HAART for the treatment of established in vivo HIV-1 infection. The viral loads in mice treated with HAART plus CD4-PE40 were also lower than those treated with HAART alone (mean, 51.7 ± 28.7 vs. 91.7 ± 26), but the difference was not statistically significant ($P = .23$). The increased in vivo activity of 3b3(Fv)-PE38 is consistent with the results of previous in vitro studies, which indicates that 3b3(Fv)-PE38 has a somewhat greater potency than CD4-PE40 [27].

Discussion

The findings of this study are the first demonstration that Env-targeted toxins have anti-HIV-1 activity in vivo. They also validate the utility of our thy/liv SCID/hu mouse system for evaluating the in vivo efficacy of different anti-HIV multidrug regimens. In particular, the emergence of HIV infection after the cessation of HAART in these mice provides an in vivo system that can be used to examine the additive anti-HIV-1 effects of various agents used in conjunction with HAART. The activities of the toxins were observed in models for both acute and established infection. However, although the toxins had prominent activity when used in conjunction with HAART, they were minimally effective when used alone. These results are consistent with 2 of our earlier findings in vitro [23, 30]: (1) CD4-PE40 only partially blocks spreading HIV infection, and (2) CD4-PE40 displays potent synergistic activity with a reverse transcriptase inhibitor; combination treatment completely eliminates infectious HIV-1 from cell cultures, an effect that was not achievable with either agent alone. The modest in vitro and in vivo effects observed with the Env-targeted toxins alone can be simply explained by their known mechanism of action; these agents can exert their anti-HIV activities only after Env has been expressed on the surface of the infected cell. Thus, complete suppression of virus spread would be expected only if the cells are killed before any progeny virions are released. Given the complex kinetic parameters governing the rates of cell killing versus virion release, it is not surprising that the toxins alone fail to completely eliminate the infected cell population before some viral spread occurs. Complementary effects might be anticipated when the toxins are combined with inhibitors of essential HIV replication enzymes because the latter agents effectively block subsequent rounds of infection by newly released virions but do not attack cells that are already infected. In the present in vivo experiments, suboptimal HAART was strongly augmented by CD4-PE40, but not by the control mixture of sCD4 plus an irrelevant PE-based toxin. This finding verifies that the complementary activity of the Env-targeted toxin was indeed due to selective killing of the HIV-infected cells. However, we cannot rule out the possibility that other anti-HIV agents with entirely different modes of action might also show complementary activities with the suboptimal HAART regimen.

The present studies are the beginning of a new effort to assess the clinical potential of complementing HAART with Env-targeted toxins, as proposed elsewhere [23]. The toxins used could be those examined in this report or similar agents developed by other investigators [21]. This modality could possibly be used

Table 2. Measurements of viral load in thy/liv-SCID-hu mice infected with human immunodeficiency virus (HIV) showing that HIV envelope (Env)–targeted toxins enhance the ability of highly active antiretroviral therapy (HAART) to suppress established HIV-1 infection in vivo.

Treatment, mouse no.	Viral load, TCID/10^4 thymocytes	
	1 mo after infection, before treatment	After 1 mo of treatment
None		
253-b5	3125	3125
259-a2	3125	3125
250-a3	3125	3125
Mean ± SEM	3125 ± 0	3125 ± 0
High-dose HAART		
255-c4	3125	125
255-c5	3125	125
255-c6	3125	25
Mean ± SEM	3125 ± 0	91.7 ± 26
High-dose HAART plus:		
CD4-PE40		
255-c2	3125	25
255-c1	3125	125
255-b6	3125	5
Mean ± SEM	3125 ± 0	51.7 ± 28.7
3B3(Fv)-PE38		
255-b2	3125	5
255-a4	3125	25
255-a3	3125	1
Mean ± SEM	3125 ± 0	10.33 ± 5.7

NOTE. The mice were injected intraperitoneally with HIV-1_{59} (8000 $TCID_{50}$). Env-target toxin was administered at a total dose of 50 ng, given in 5 doses on alternate days starting 3 weeks after the initiation of HAART.

to prevent the establishment of persistent HIV-1 infection in individuals presenting soon after HIV-1 exposure (e.g., newborns of infected mothers; postexposure prophylaxis). Moreover, Env-targeted toxins may serve to help eliminate reservoirs of infected cells that persist after years of HAART; these reservoirs include latently infected resting $CD4^+$ memory T cells in the circulation and lymphoid tissue [26], blood and lymphoid cells responsible for the virus replication that persists after HAART [4, 8–16], and perhaps other cell types and tissue compartments that are refractory to HAART [7].

Latently infected cells are a particularly difficult problem. It has been proposed that the latent reservoirs may be flushed out by deliberate treatment with agents that activate latently infected cells [4]. Indeed, supplementing HAART with intermittent IL-2 therapy has been shown to significantly reduce the pool of latently infected resting $CD4^+$ T cells in blood and lymph nodes [31]. However, the IL-2 treatment had negligible effect on the viral load rebound after cessation of therapy [19]. We propose that in such protocols, the Env-targeted toxins may effectively kill the newly activated cells, because these cells should be induced to express surface Env. However, we note that the toxins will be beneficial only if they accelerate the natural mechanisms governing the decline of persistent virus-producing cells (i.e., intrinsic cellular decay rates, viral cytopathic effects, and immune effector mechanisms such as cytotoxic T cells).

Another critical issue for using Env-targeted toxins in conjunction with HAART is the dose-limiting hepatotoxicity observed with CD4-PE40 in earlier phase I trials. This problem is perplexing for several reasons. First, dose-limiting hepatotoxicity was observed in HIV-1–infected people (maximum tolerated dose [MTD] 10 μg/kg, [24, 25]) but was not seen in preclinical toxicology studies with uninfected rodents and nonhuman primates (MTD 250 μg/kg; unpublished results). Second, in recent phase I trials for tumor therapy, different PE-based immunotoxins have been well tolerated, and significant antitumor activity was observed at tolerable doses (20–40 μg/kg) without serious hepatotoxicity ([32]; R. Kreitman, L. Pai-Scherf, and I. Pastan, unpublished results). Thus, the dose-limiting hepatotoxicity previously observed with CD4-PE40 appears to be unique to the use of this chimeric toxin in HIV-1–infected individuals. We have suggested [23] that this problem may have resulted from the high viral loads in subjects treated in the pre-HAART era. Specifically, we proposed that soluble gp120 shed from virions or infected cells would bind to circulating CD4-PE40; the resulting complexes would be delivered to the liver by several mechanisms. If this notion is valid, then hepatotoxicity should not pose a problem under conditions of HAART-mediated virus suppression. Alternatively, if the hepatotoxicity is a unique feature of CD4-PE40 in humans, then immunotoxins such as 3b3(Fv)-PE38 should not be problematic, particularly in view of the absence of severe hepatotoxicity with other PE-based antitumor immunotoxins in phase I trials, as noted earlier. The in vivo results presented here provide an impetus for diverse lines of experimentation, both for in vitro and animal models, to evaluate these critical issues. Such efforts may help pave the way for effective clinical efforts to eradicate HIV-1 infection from the body.

References

1. Saag MS, Schooley RT. Antiretroviral chemotherapy. Curr Clin Top Infect Dis 1998;18:154–79.
2. Wong JK, Hezareh M, Gunthard HF, et al. Recovery of replication competent HIV despite prolonged suppression of plasma viremia. Science 1997;278: 1291–5.
3. Finzi D, Hermankova M, Pierson T, et al. Identification of a reservoir for HIV1 in patients on highly active antiretroviral therapy. Science 1997; 278:1295–300.
4. Chun TW, Stuyver L, Mizell SB, et al. Presence of an inducible HIV1 latent reservoir during highly active antiretroviral therapy. Proc Natl Acad Sci USA 1997;94:13193–7.
5. Chun TW, Engel D, Berrey MM, Shea T, Corey L, Fauci AS. Early establishment of a pool of latently infected, resting $CD4^+$ T cells during primary HIV1 infection. Proc Natl Acad Sci USA 1998;95:8869–73.
6. Finzi D, Blankson J, Siliciano JD, et al. Latent infection of $CD4^+$ T cells provides a mechanism for lifelong persistence of HIV1, even in patients on effective combination therapy. Nat Med 1999;5:512–7.
7. Zhang H, Dornadula G, Beumont M, et al. Human immunodeficiency virus type 1 in the semen of men receiving highly active antiretroviral therapy. N Engl J Med 1998;339:1803–9.
8. Cavert W, Notermans DW, Staskus K, et al. Kinetics of response in lymphoid

tissues to antiretroviral therapy of HIV1 infection. Science 1997;276: 960–4.

9. Natarajan V, Bosche M, Metcalf JA, Ward DJ, Lane HC, Kovacs JA. HIV1 replication in patients with undetectable plasma virus receiving HAART. Lancet 1999;353:119–20.
10. Martinez MA, Cabana M, Ibanez A, Clotet B, Arno A, Ruiz L. Human immunodeficiency virus type 1 genetic evolution in patients with prolonged suppression of plasma viremia. Virology 1999;256:180–7.
11. Zhang L, Ramratnam B, Tenner-Racz K, et al. Quantifying residual HIV1 replication in patients receiving combination antiretroviral therapy. N Engl J Med 1999;340:1605–13.
12. Furtado MR, Callaway DS, Phair JP, et al. Persistence of HIV1 transcription in peripheral blood mononuclear cells in patients receiving potent antiretroviral therapy. N Engl J Med 1999;340:1614–22.
13. Hockett RD, Kilby JM, Derdeyn CA, et al. Constant mean viral copy number per infected cell in tissues regardless of high, low, or undetectable plasma HIV RNA. J Exp Med 1999;189:1545–54.
14. Gunthard HF, Frost SDW, Leigh-Brown AJ, et al. Evolution of envelope sequences of human immunodeficiency virus type 1 in cellular reservoirs in the setting of potent antiviral therapy. J Virol 1999;73:9404–12.
15. Dornadula G, Zhang H, VanUitert B, et al. Residual HIV1 RNA in blood plasma of patients taking suppressive highly active antiretroviral therapy. JAMA 1999;282:1627–32.
16. Zhang ZQ, Schuler T, Zupancic M, et al. Sexual transmission and propagation of SIV and HIV in resting and activated CD4$^+$ T cells. Science 1999;286:1353–7.
17. Montaner JSG, Harris M, Mo T, Harrigan PR. Rebound of plasma HIV viral load following prolonged suppression with combination therapy. AIDS 1998;12:1398–9.
18. Jubault V, Burgard M, Le Corfec E, Costagliola D, Rouzioux C, Viard JP. High rebound of plasma and cellular HIV load after discontinuation of triple combination therapy. AIDS 1998;12:2358–9.
19. Chun TW, Davey RT, Engel D, Lane HC, Fauci AS. Reemergence of HIV after stopping therapy. Nature 1999;401:874–5.
20. Neumann AU, Tubiana R, Calvez V, et al. HIV1 rebound during interruption of highly active antiretroviral therapy has no deleterious effect on reinitiated treatment. AIDS 1999;13:677–83.
21. Pincus SH. Therapeutic potential of antiHIV immunotoxins. Antiviral Res 1996;33:1-9.
22. Chaudhary VK, Mizukami T, Fuerst TR, et al. Selective killing of HIV infected cells by recombinant human CD4-*Pseudomonas* exotoxin hybrid protein. Nature 1988;335:369–72.
23. Berger EA, Moss B, Pastan I. Reconsidering targeted toxins to eliminate HIV infection: you gotta have HAART. Proc Natl Acad Sci USA 1998;95: 11511–3.
24. Ramachandran RV, Katzenstein DA, Wood R, Batts DH, Merigan TC. Failure of short term CD4PE40 infusions to reduce virus load in human immunodeficiency virus infected persons. J Infect Dis 1994;170:1009–13.
25. Davey RT, Boenning CM, Herpin BR, et al. Use of recombinant soluble CD4 Pseudomonas exotoxin, a novel immunotoxin, for treatment of persons infected with human immunodeficiency virus. J Infect Dis 1994;170: 1180–8.
26. Pettoello-Mantovani M, Kollmann TR, Katopodis NF, et al. Thy/livSCIDhu mice: a system for investigating the in vivo effects of multidrug therapy on plasma viremia and human immunodeficiency virus replication in lymphoid tissues. J Infect Dis 1998;177:337–46.
27. Bera TK, Kennedy PE, Berger EA, Barbas CF III, Pastan I. Specific killing of HIV infected lymphocytes by a recombinant immunotoxin directed against the HIV1 envelope glycoprotein. Mol Med 1998;4:384–91.
28. Kreitman RJ, Wang QQ, Fitzgerald DJP, Pastan I. Complete regression of human B cell lymphoma xenografts in mice treated with recombinant antiCD22 immunotoxin RFB4(dsFv)PE38 at doses tolerated by cynomolgus monkeys. Int J Cancer 1999;81:148–55.
29. Kollmann TR, Kim A, Pettoello-Mantovani M, et al. Divergent effects of chronic HIV1 infection on human thymocyte maturation in SCIDhu mice. J Immunol 1995;154:907–921.
30. Ashorn P, Moss B, Weinstein JN, et al. Elimination of infectious human immunodeficiency virus from human T cell cultures by synergistic action of CD4-*Pseudomonas* exotoxin and reverse transcriptase inhibitors. Proc Natl Acad Sci USA 1990;87:8889–93.
31. Chun TW, Engel D, Mizell SB, et al. Effect of interleukin2 on the pool of latently infected, resting CD4$^+$ T cells in HIV1 infected patients receiving highly active antiretroviral therapy. Nat Med 1999;5:651–5.
32. Kreitman RJ, Wilson WH, Robbins D, et al. Responses in refractory hairy cell leukemia to a recombinant immunotoxin. Blood 1999;94:3340–8.

1: Nature 1984 Feb 16-22;307(5952):650-2

Related Articles, Links

Mapping by monoclonal antibody detection of glycosaminoglycans in connective tissues.

Couchman JR, Caterson B, Christner JE, Baker JR.

Chondroitin sulphate proteoglycans are widespread connective tissue components and chemical analysis of cartilage and other proteoglycans has demonstrated molecular speciation involving the degree and position of sulphation of the carbohydrate chains. This may, in turn, affect the properties of the glycosaminoglycan (GAG), particularly with respect to self-association and interactions with other extracellular matrix components. Interactions with specific molecules from different connective tissue types, such as the collagens and their associated glycoproteins, could be favoured by particular charge organizations on the GAG molecule endowed by the sulphate groups. So far, it has not been possible to identify and map chondroitins of differing sulphation in tissues, but we have now raised three monoclonal antibodies which specifically recognize unsulphated, 4-sulphated and 6-sulphated chondroitin and dermatan sulphate. These provide novel opportunities to study the in vivo distribution of chondroitin sulphate proteoglycans. We demonstrate that chondroitin sulphates exhibit remarkable connective tissue specificity and furthermore provide evidence that some proteoglycans may predominantly carry only one type of chondroitin sulphate chain.

PMID: 6420711 [PubMed - indexed for MEDLINE]

Display Abstract Show: 20 Sort Send to Text

Proc. Natl. Acad. Sci. USA
Vol. 88, pp. 10134–10137, November 1991
Medical Sciences

A large array of human monoclonal antibodies to type 1 human immunodeficiency virus from combinatorial libraries of asymptomatic seropositive individuals

(AIDS/antibody repertoires/passive immunization/filamentous phage/phage surface expression)

DENNIS R. BURTON*†, CARLOS F. BARBAS III*, MATS A. A. PERSSON*‡, SCOTT KOENIG§, ROBERT M. CHANOCK¶, AND RICHARD A. LERNER*

*Departments of Molecular Biology and Chemistry, Scripps Research Institute, 10666 North Torrey Pines Road, La Jolla, CA 92037; §Laboratory of Immunoregulation and ¶Laboratory of Infectious Diseases, National Institute of Allergy and Infectious Diseases, National Institutes of Health, Bethesda, MD 20892; †Krebs Institute, Department of Molecular Biology and Biotechnology, The University of Sheffield, Sheffield S10 2TN, United Kingdom; and ‡Department of Medicine, Karolinska Institute, Karolinska Hospital, Box 60500, S-104 01 Stockholm, Sweden

Contributed by Richard A. Lerner, August 22, 1991

ABSTRACT **A panel of human monoclonal antibody Fab fragments has been generated against the surface glycoprotein gp120 of type 1 human immunodeficiency virus (HIV) by antigen selection from a random combinatorial library expressed on the surface of filamentous phage. The library was prepared from 5 ml of bone marrow from an asymptomatic individual who has been HIV-positive for 6 years. The antibodies have high affinity for antigen (mostly with affinity constants of $>10^8$ M^{-1}) and notable sequence diversity. Given appropriate donor selection, the methods described should allow the generation of antibodies for the evaluation of passive immunization as a therapy for AIDS.**

Counter-AIDS strategies that are under intensive scrutiny include passive immunization to slow or halt the progression of human immunodeficiency virus (HIV) infection in seropositive individuals and vaccination to prevent infection. Both approaches could greatly benefit from the generation of large numbers of human HIV-specific monoclonal antibodies.

There is increasing evidence that passive immunization could be an effective strategy for the treatment and prophylaxis of the disease. Two groups have reported clinical benefit in patients with AIDS who were given plasma from healthy asymptomatic HIV-positive donors (1, 2). In the former case the plasma was known to contain high anti-HIV neutralizing titer. Two other groups have described a correlation between the presence of maternal antibodies against select epitopes of viral envelope glycoprotein gp120 and the failure of infected mothers to transmit the virus to their offspring (3–5). The appropriate passively transferred antibodies have also been shown effective in preventing HIV infection in chimpanzees (6) and in preventing HIV-2 and simian immunodeficiency virus (SIV) infection in cynomolgus monkeys (7).

Although many murine and a few human antibodies to HIV exist (for a recent review, see ref. 8), a broad-based program to evaluate the utility of antibodies in combatting HIV infection will likely require the facile generation of large panels of human anti-HIV antibodies. There are a number of reasons for this. First, the antibodies would need to be administered repeatedly over an extended period of time and so should not only be human to avoid anti-antibody (typically anti-rodent) responses but also be available in a number of idiotypic forms with retention of activity to avoid anti-idiotypic responses. Second, the broad spectrum of viral strains means that the generation of single or even small numbers of monoclonal antibodies against the virus is unlikely to suffice. Third, it may be necessary to examine many antibodies to find rare but highly effective molecules. Antibodies could be rare either because they are present as minor components of typical responses or because they are present in only a few individuals.

Similarly, the study of large numbers of human antibodies should accelerate vaccine design. Recent vaccination data in nonhuman primates have shown the development of protective immunity against HIV-1 in chimpanzees vaccinated with recombinant gp120 (9) and against HIV-2 in cynomolgus monkeys vaccinated with whole killed virus (10). These studies raise a number of important issues. For instance, the former report found that gp160, which includes the full gp120 molecule, was not protective. Given that antibodies are believed to be key in protective immunity (9), the molecular dissection of human antibody responses to HIV should allow assessment of the utility of protective epitopes in the context of the natural host.

Conventional technologies for antibody generation, such as hybridomas and Epstein–Barr virus transformation (11), cannot readily meet the challenge of assessing large numbers of human monoclonal antibodies from HIV-infected individuals at various stages of their clinical course. Our approach to the problem has been to prepare random combinatorial libraries. Initially, antigen binders were selected from libraries constructed using phage λ vectors (12). This method worked well for immunized mice (12, 13) and for "boosted" humans (14, 15), but we were unable to prepare specific antibodies from HIV-infected individuals. Recent papers have described the expression of random combinatorial antibody libraries on the surface of M13 phage and have shown how this allows much more rapid selection of specific antibodies from larger libraries (16, 17). Here we report that this method can be used to generate large panels of specific viral antibodies from the lymphocytes of HIV-positive individuals.‖

MATERIALS AND METHODS

Lymphocyte RNA Preparation. Five milliliters of bone marrow was removed by aspiration from HIV-1-positive donors. Immediately, 10 ml of 3 M guanidinium isothiocyanate containing 71 μl of 2-mercaptoethanol was added and then RNA was prepared by the standard method (18).

The publication costs of this article were defrayed in part by page charge payment. This article must therefore be hereby marked "*advertisement*" in accordance with 18 U.S.C. §1734 solely to indicate this fact.

Abbreviations: BSA, bovine serum albumin; CDR, complementarity-determining region; HIV, human immunodeficiency virus.

‖The sequences reported in this paper have been deposited in the GenBank data base (accession nos. M80715–M80734).

Library Construction. Total RNA (typically 10 μg) was reverse-transcribed and γ1 (Fd region) and κ chains were amplified by PCR as described (14). The resulting γ1 heavy-chain DNA was cut with an excess of the restriction enzymes *Xho* I and *Spe* I and typically about 350 ng was ligated with 2 μg of *Xho* I/*Spe* I-linearized pComb3 vector (isolated by agarose gel electrophoresis) in a total volume of 150 μl with 10 units of ligase (BRL) at 16°C overnight. Following ligation, DNA was precipitated at −20°C for 2 hr by the addition of 2 μl of 2% (wt/vol) glycogen, 15 μl of 3 M sodium acetate (pH 5.2), and 330 μl of ethanol. DNA was pelleted by microcentrifugation at 4°C for 15 min. The DNA pellet was washed with cold 70% ethanol and dried under vacuum. The pellet was resuspended in 10 μl of water and transformed by electroporation into 300 μl of *Escherichia coli* XL1-Blue (16). After transformation, 3 ml of SOC medium (16) was added and the culture was shaken at 220 rpm for 1 hr at 37°C after which 10 ml of SB (super broth; 30 g of tryptone, 20 g of yeast extract, and 10 g of Mops per liter, pH 7) containing carbenicillin (20 μg/ml) and tetracycline (10 μg/ml) was added. At this point, samples (20, 1, and 0.1 μl) were withdrawn for plating to determine the library size. Typically the library had about 10^7 members. The culture was grown for an additional hour at 37°C while shaking at 300 rpm. This culture was added to 100 ml of SB containing carbenicillin (50 μg/ml) and tetracycline (10 μg/ml) and was grown overnight. Phagemid DNA containing the heavy-chain library was prepared from this overnight culture. To determine the insert frequency of this ligation, 10 colonies from the plates used to titer the library were picked and grown. DNA was prepared and then digested with *Xho* I and *Spe* I.

For the cloning of the light chain, phagemid DNA (10 μg) was digested as described above except that the restriction enzymes *Sac* I and *Xba* I were used. The resulting linearized vector was treated with phosphatase and purified by agarose gel electrophoresis. The desired fragment, 4.7 kilobases long, was excised from the gel. Ligation of this vector with prepared light-chain PCR DNA proceeded as described above for the heavy chain. After transformation, 3 ml of SOC medium was added and the culture was shaken at 220 rpm for 1 hr at 37°C. Then 10 ml of SB containing carbenicillin (20 μg/ml) and tetracycline (10 μg/ml) was added (samples were removed for titering as described above for the heavy-chain cloning) and the culture was shaken at 300 rpm for an additional hour. This culture was added to 100 ml of SB containing carbenicillin (50 μg/ml) and tetracycline (10 μg/ml) and then shaken for 1 hr. Helper phage VCS-M13 (10^{12} plaque-forming units) was added and the culture was shaken for an additional 2 hr. After this time, kanamycin (70 μg/ml) was added and the culture was incubated at 37°C overnight. The supernatant was cleared by centrifugation (4000 rpm for 15 min in a JA-10 rotor) at 4°C. Phage were precipitated by addition of 4% (wt/vol) polyethylene glycol 8000 and 3% (wt/vol) NaCl followed by incubation on ice for 30 min and centrifugation. Phage pellets were resuspended in 2 ml of phosphate-buffered saline (PBS: 50 mM phosphate, pH 7.2/150 mM NaCl) and microcentrifuged for 3 min to pellet debris. Supernatants were transferred to fresh tubes and stored at −20°C.

Titering of Colony-Forming Units. Phagemids that have been packaged into virions are capable of infecting male *E. coli* to form colonies on selective plates. Phage (packaged phagemid) was diluted in SB (dilutions: 10^{-3}, 10^{-6}, and 10^{-8}) and 1 μl was used to infect 50 μl of fresh *E. coli* XL1-Blue culture (OD_{600} = 1) grown in SB containing tetracycline (10 μg/ml). Phage and cells were incubated at room temperature for 15 min and then directly plated on LB/carbenicillin plates.

Panning of the C mbinatorial Library t Select Antigen Binders. The panning procedure is a modification of that originally described by Parmley and Smith (19). Four wells of a microtiter plate (Costar 3690) were coated overnight at 4°C with 25 μl of antigen (40 μg/ml in 0.1 M bicarbonate buffer, pH 8.6). The wells were washed twice with water and blocked by completely filling the well with 1% (wt/vol) bovine serum albumin (BSA) in PBS and incubating the plate at 37°C for 1 hr. Blocking solution was shaken out, 50 μl of the phage library (typically 10^{11} colony-forming units) was added to each well, and the plate was incubated at 37°C for 2 hr. Phage were removed and the plate was washed once with water. Each well was then washed 10 times with 50 mM Tris·HCl, pH 7.5/150 mM NaCl/0.5% Tween 20 over a period of 1 hr at room temperature. The plate was washed once more with distilled water and adherent phage were eluted by the addition of 50 μl of elution buffer (0.1 M HCl, adjusted to pH 2.2 with solid glycine and containing 0.1% BSA) to each well and incubation at room temperature for 10 min. The elution buffer was pipetted up and down several times, removed, and neutralized with 3 μl of 2 M Tris base per 50 μl of elution buffer used. Eluted phage were used to infect 2 ml of fresh *E. coli* XL1-Blue cells (OD_{600} = 1) for 15 min at room temperature after which 10 ml of SB containing carbenicillin (20 μg/ml) and tetracycline (10 μg/ml) was added. Samples (20, 1, and 0.1 μl) were removed for plating to determine the number of phage (packaged phagemids) that were eluted from the plate. The culture was shaken for 1 hr at 37°C and then added to 100 ml of SB containing carbenicillin (50 μg/ml) and tetracycline (10 μg/ml) and shaken for 1 hr. Helper phage VCS-M13 (10^{12} plaque-forming units) were added and the culture shaken for an additional 2 hr. Then kanamycin (70 μg/ml) was added and the culture was incubated at 37°C overnight. Phage preparation and further panning were repeated as described above.

Following each round of panning, the percent yield of phage was determined as (no. of phage eluted/no. of phage applied) × 100.

Preparation of Soluble Fab Fragments. Phagemid DNA from positive clones was isolated and digested with *Spe* I and *Nhe* I. Digestion with these enzymes produces compatible cohesive ends. The 4.7-kilobase DNA fragment lacking the gene III portion was gel-purified (0.6% agarose) and self-ligated.

Transformation of *E. coli* XL1-Blue afforded the isolation of recombinants lacking the gene III fragment. Clones were examined for removal of the gene III fragment by *Xho* I/*Xba* I digestion, which yielded a 1.6-kilobase fragment. Clones were grown in 15 ml of SB containing carbenicillin (50 μg/ml) and 20 mM $MgCl_2$ at 37°C until OD_{600} of 0.2 was achieved.

Isopropyl β-D-thiogalactopyranoside (1 mM) was added and the culture was incubated overnight at 37°C. Cells were pelleted by centrifugation at 4000 rpm for 15 min in a JA-10 rotor (Beckman J2-21) at 4°C. Cells were resuspended in 3 ml of PBS containing 0.2 mM phenylmethylsulfonyl fluoride and lysed by sonication on ice (2–4 min, 50% duty). The debris was pelleted by centrifugation at 14,000 rpm in a JA-20 rotor at 4°C for 15 min. The supernatant was used directly for ELISA analysis and was stored at −20°C.

ELISA Analysis of Fab Supernatants. ELISA wells were coated with gp120 exactly as above, washed five times with water, blocked in 100 μl of 1% BSA/PBS for 1 hr at 37°C, and then incubated with 25 μl Fab supernatants for 1 hr at 37°C. After 10 washes with water, 25 μl of a 1:1000 dilution of alkaline phosphatase-conjugated goat anti-human IgG $F(ab')_2$ (Pierce) was added and incubated for 1 hr at 37°C. Following 10 washes with water, 50 μl of *p*-nitrophenyl phosphate substrate was added and color development was monitored at 405 nm. Positive clones gave A_{405} values of >1 (mostly >1.5) after 10 min, whereas negative clones gave values of 0.1–0.2.

Inhibition ELISAs. Affinity measurement was carried out by inhibition ELISAs (20). Microtiter wells were coated with

gp120 (5 μg/ml in 0.1 M bicarbonate buffer, pH 8.6) overnight at 4°C. The wells were blocked with 1% BSA/PBS for 1 hr at 37°C. Dilutions of the samples previously determined in titration experiments to result in substantial reduction of OD values after 2-fold dilution (i.e., arranged on the "slope" of the titration curve) were mixed with free gp120 in the wells at a final concentration of 10^{-7} to 10^{-11} M in 0.5% BSA/0.025% Tween 20/PBS. The plates were incubated for 90–120 min at 37°C and carefully washed 10 times with 0.05% Tween 20/PBS before addition of goat anti-human IgG F(ab')$_2$ at a dilution of 1:500. After 1 hr of incubation and washes as above, *p*-nitrophenyl phosphate was added as substrate (Sigma). Plates were read at 405 nm after 15 min.

Nucleic Acid Sequencing. Nucleic acid sequencing was carried out on double-stranded DNA with Sequenase 1.0 (United States Biochemical).

RESULTS AND DISCUSSION

Previously work has shown that the antibody phage surface expression system can be successfully used to isolate specific antibodies occurring in a combinatorial library at a frequency of about 1 in 5000 (16). Two rounds of antigen panning of a library prepared from an individual boosted with tetanus toxoid were sufficient to enrich the library to the extent that 27 out of 38 clones expressed tetanus toxoid-specific antibody following panning. In other studies a library was prepared that included known anti-tetanus toxoid antibody clones at a frequency of about 1 in 170,000. Three rounds of panning against toxoid were found to give enrichment such that 20/20 clones were antigen-specific, indicating that the method could access clones of low abundance from combinatorial libraries. This improved methodology for screening combinatorial libraries encouraged us to return to the HIV problem.

Libraries from a number of asymptomatic HIV positive donors have been prepared. We report now on the first donor studied, a 31-year-old homosexual male who has been HIV-positive for 6 years but has no symptoms of disease. Serological studies showed the presence of a significant ELISA titer (1:3000) against the HIV-1 surface glycoprotein gp120. After informed consent was given by the donor, bone marrow cells were obtained by aspiration. RNA was isolated from the lymphocytes and heavy (γ1, Fd region)- and light (κ)-chain genes amplified from the corresponding cDNAs by the PCR. The antibody genes were then cloned into the M13 phage surface expression vector pComb3 to give a library of 10^7 members.

The phage surface expression library was panned against recombinant gp120 (strain IIIB) coated on ELISA wells. Four rounds of panning produced an ≈100-fold amplification in eluted phage, indicating enrichment for specific antigen-binding clones. In the first panning, 4.6×10^{11} phage were applied to four wells and 7.7×10^5 phage were eluted. After the fourth panning 1.0×10^8 phage were eluted. Eluted phage were used to infect *E. coli* XL1-Blue cells. DNA was prepared from these cells, cut with *Nhe* I and *Spe* I to remove the gene III fragment, and religated. The reconstructed phagemid was used to transform XL1-Blue cells to produce clones secreting soluble Fab fragments. Forty such clones were grown up and the supernatants, containing Fab fragments, were screened in an ELISA for reactivity with recombinant gp120. The supernatants from 33 clones showed clear reactivity. The supernatants did not react with BSA-coated wells, and anti-tetanus toxoid Fab supernatants did not react with gp120-coated wells.

DNA samples from the reactive 33 clones were used as templates for sequencing of thymidine nucleotides of the variable regions of the heavy and light chains to reveal that at least 10 clones had unique heavy chains and 20 clones unique light chains. A representative number of chains were then sequenced. Fig. 1 compares the CDR3 sequences of these heavy and light chains and indicates the diversity of the panel of antibodies cloned. The details of the response to gp120 will be discussed elsewhere. Here we briefly note that clones identical with respect to heavy-chain CDR3 but differing in light-chain CDR3 sequences (e.g., nos. 14 and 31) were observed, as well as clones that were identical in both chains (e.g., nos. 11 and 29). The former is an example of chain promiscuity, which may be useful in altering idiotypy while retaining specificity (21).

To measure the affinities of the Fab fragments for gp120, inhibition ELISAs using soluble gp120 were performed. As shown in Fig. 2, most inhibition constants were $<10^{-8}$ M, implying monomer Fab–gp120 binding constants of the order of or greater than 10^8 M^{-1}.

The gp120 used in these experiments was derived from the IIIB strain for reasons of availability. However, this strain is thought to be very rare in the United States (22) and therefore it is likely that most of the antibodies we have selected are strain-crossreactive. Indeed, initial studies indicate that the binding of a number of the Fab fragments to gp120 is inhibited

LIGHT CHAIN				HEAVY CHAIN			
Clone	FR3	CDR3	FR4	Clone	FR3	CDR3	FR4
3	YYC	QQYGDSPLYS	FGQG	3	YYCAT	KYPRYSDMVTGVRNHFYMDV	WGKG
7	YYC	QQYGSSRYT	FGQG	7	YYCAR	VGPYTWDDSPQDNYYMVV	WGKG
11	YYC	QQFGDAQYT	FGQG	11	YYCAT	RYPRYSEMMGGVRKHFYMDV	WGKG
14	YYC	QKYQSAPRT	FGQG	14	YYCAR	ERRERGWNPRALRGALDF	WGQG
20	YYC	QNYDSAPWT	FGQG	20	YYCAT	QKPRYFDLLSGQYRRVAGAFDV	WGHG
21	YYC	QVYGASSYT	FGQG	21	YYCAR	VGPYTWDDSPQDNYYMDV	WGKG
22	YYC	QQSYSTPYT	FGQG	22	YYCAR	DIGLKGEHYDILTAYGPDY	WGQG
24	YSC	QQYGTSPWT	FGQG	24	YFCAR	ERRERGWNPRALRGALEV	WGQG
29	YYC	QQFGDAQYT	FGQG	29	YYCAT	RYPRYSEMMGGVRKHFYMDV	WGKG
31	YYC	QKYNSAPRT	FGQG	31	YYCAR	ERRERGWNPRALRGALDF	WGQG

FIG. 1. Amino acid sequences of heavy- and light-chain complementarity-determining region 3 (CDR3) from HIV gp120-binding clones. The flanking sequences of the framework regions FR3 and FR4 are also shown.

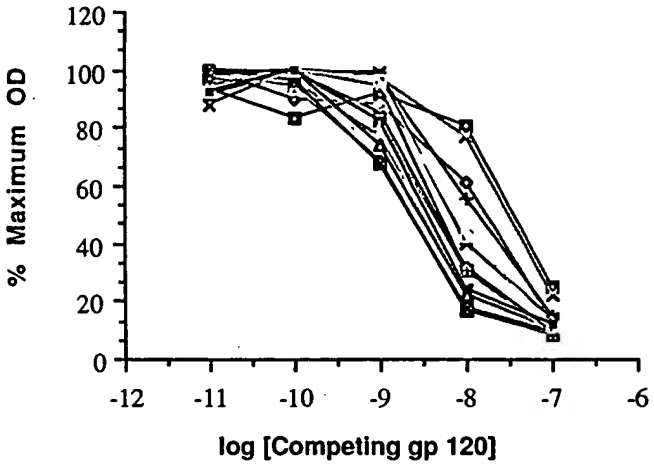

FIG. 2. Affinities of Fab fragments for gp120, estimated by inhibition ELISA for 15 different clones.

by soluble CD4, suggesting that they may recognize the CD4 interaction site.

The phage surface library was also panned against the HIV glycoprotein gp160. After four rounds of panning a 200-fold enrichment was observed. Supernatants containing soluble Fab fragments were then screened in an ELISA against gp160 and gp120. Of 35 clones reacting with gp160, 8 reacted also with gp120. The remainder are likely to be against gp41 or epitopes on gp120 that are sensitive to the presence of gp41. Screening against gp41 peptides may be useful in distinguishing these possibilities.

For generation of the present library, we have focused only on antibodies from the major heavy-chain variable-region subgroup families and κ light chains. Yet, from only 5 ml of bone marrow we have been able to obtain a large panel of high-affinity antibodies against HIV. This study, along with several others (12–16, 23), stands in contrast to theoretical arguments that the chances of isolating high-affinity antibodies from random combinatorial libraries were "remote" (24). As previously pointed out (15), the fact that libraries are constructed from immunologically amplified mRNA and not DNA is a crucial fact in any calculations concerning the probability of obtaining the original pairings of heavy and light chains. Immunized animals give libraries rich in functional chains that are recombined with one another relatively frequently to generate high-affinity antibodies, many of which probably represent the original *in vivo* pairings. In a real sense, by its sensitivity to mRNA, the combinatorial approach is reporting on the current antibody response of the donor.

The sensitivity of the method in combination with cell enrichment techniques should also allow us to draw upon the "fossil record" of the antibody response of an individual. This may be important in situations where immunological competence has deteriorated such as in AIDS or aging. For example, in AIDS we may wish to resurrect antibodies from different times in the host–virus encounter, for either analytical or therapeutic purposes (25).

At any rate, after addition of the Fc region, human antibodies from combinatorial libraries could form the basis of clinical trials of the efficacy of passive immunization in AIDS. While the present studies constitute a proof of principle, for trials of passive immunization in patients it will be necessary to decide what donor(s), how many antibodies, and which specificities should be used.

We are particularly grateful to the donor for his cooperation. We acknowledge considerable assistance from Roger Caothien, Doug Cababa, John Dickson, Eva von Garrelts, Denise Hoekstra, Terri Jones, Loren Peterson, and Anthony Williamson. We thank Sydney Brenner, Norton B. Gilula, Nicola Green, and Angray Kang for critical review of the manuscript. We acknowledge the financial support of Johnson & Johnson, Public Health Service Grant IP50 MH47680, the Sven and Dagmar Salén Foundation, and The Swedish Cancer Fund. D.R.B. is a Jenner Fellow of the Lister Institute of Preventive Medicine.

1. Jackson, G. G., Perkins, J. T., Rubenis, M., Paul, D. A., Knigge, M. & Despotes, J. C. (1988) *Lancet* ii, 647–652.
2. Karpas, A., Hill, F., Youle, M., Cullen, V., Gray, J., Byron, N., Hayhoe, F., Tenent-Flowers, M., Howard, L., Gilgen, D., Oates, J. K., Hawkins, D. & Gazzard, B. (1988) *Proc. Natl. Acad. Sci. USA* **85**, 9234–9237.
3. Rossi, P., Moschese, V., Broliden, P. A., Fundaro, C., Quinti, I., Plebani, A., Giaquinto, C., Tovo, P. A., Ljunggren, K., Rosen, J., Wigzell, H., Jondal, M. & Wahren, B. (1989) *Proc. Natl. Acad. Sci. USA* **86**, 8055–8058.
4. Goedert, J. J., Drummond, J. E., Minkoff, H., Stevens, R., Blattner, W., Mendez, H., Robert-Guroff, M., Holman, S., Rubinstein, A., Willoughby, A. & Landesmann, S. H. (1991) *Lancet* **337**, 1351–1354.
5. Devash, Y., Calvell, T. A., Wood, D. G., Reagan, K. J. & Rubinstein, A. (1990) *Proc. Natl. Acad. Sci. USA* **87**, 3445–3449.
6. Emini, E. A., Nara, P. L., Shleiff, W. A., Lewis, J. A., Davide, J. P., Lee, R. D., Kessler, J., Conley, S., Matsushita, S., Putney, S. D., Gerety, R. J. & Eichberg, J. W. (1990) *J. Virol.* **64**, 3674–3678.
7. Putkonen, P., Thorstensson, R., Ghavamzadeh, L., Albert, J., Hild, K., Biberfeld, G. & Norrby, E. *Nature (London)* **352**, 436–438.
8. Nara, P. L., Garrity, R. R. & Goudsmit, J. (1991) *FASEB J.* **5**, 2437–2455.
9. Berman, P. W., Gregory, T. J., Riddle, L., Nakamura, G. R., Champe, M. A., Porter, J. P., Wurm, F. M., Hershberg, R. D., Cobb, E. K. & Eichberg, J. W. (1990) *Nature (London)* **345**, 622–625.
10. Putkonen, P., Thorstensson, R., Walther, L., Albert, J., Åkerblom, L., Granquist, G., Wadell, G., Norrby, E. & Biberfeld, G. (1991) *AIDS Res. Hum. Retrovir.* **7**, 271–277.
11. James, K. & Bell, G. T. (1987) *J. Immunol. Methods* **100**, 15–40.
12. Huse, W. D., Sastry, L., Iverson, S. A., Kang, A. S., Alting-Mees, M., Burton, D. R., Benkovic, S. J. & Lerner, R. A. (1989) *Science* **246**, 1275–1281.
13. Caton, A. J. & Koprowski, H. (1990) *Proc. Natl. Acad. Sci. USA* **87**, 6450–6454; correction (1991) **88**, 1590.
14. Persson, M. A. A., Caothien, R. H. & Burton, D. R. (1991) *Proc. Natl. Acad. Sci. USA* **88**, 2432–2436.
15. Burton, D. R. (1991) *Trends Biotechnol.* **9**, 169–175.
16. Barbas, C. F., Kang, A. S., Lerner, R. A. & Benkovic, S. J. (1991) *Proc. Natl. Acad. Sci. USA* **88**, 7978–7982.
17. Kang, A. S., Barbas, C. F., Benkovic, S. J. & Lerner, R. A. (1991) *Proc. Natl. Acad. Sci. USA* **88**, 4363–4366.
18. Chomczynski, P. & Sacchi, N. (1987) *Anal. Biochem.* **162**, 156–159.
19. Parmley, S. F. & Smith, G. P. (1988) *Gene* **73**, 305–318.
20. Rath, S., Stanley, C. M. & Steward, M. W. (1988) *J. Immun. Methods* **106**, 245–249.
21. Kang, A. S., Jones, T. M. & Burton, D. R. (1991) *Proc. Natl. Acad. Sci. USA*, in press.
22. Goudsmit, J., Back, N. K. T. & Nara, P. L. (1991) *FASEB J.* **5**, 2427–2436.
23. Clackson, T., Hoogenboom, H. R., Griffiths, A. D. & Winter, G. (1991) *Nature (London)* **352**, 624–628.
24. Winter, G. & Milstein, C. (1991) *Nature (London)* **349**, 293–299.
25. Lerner, R. A., Barbas, C. F., Kang, A. S. & Burton, D. R., *Proc. Natl. Acad. Sci. USA*, in press.

mutations (DDPAC (2 brains), ManF23 and Aus1) and 3 were from families with the P301L point mutant (FTD003 (2 brains) and HFTD1). Reverse transcription was performed using the Superscript preamplification kit (Life Technologies) on 1–4 μg of brain RNA with an oligo(dT) primer. PCR was performed between exon 9 (forward, 5′-ATCGCAGCGGCTACAGCAG-3′) and exon 11 (reverse, 5′-TGGTTTATGATGGATGTTGCC-3′) and between exon 9 and exon 13 (reverse 5′-TCTTGGCTTTGGCGTTCTC-3′). In each case, the 5′ end of the forward amplification primer was labelled with TET (Perkin Elmer) to allow detection by an ABI377 automated sequencer. Preliminary PCRs (not shown) were performed using a range of amplification cycles (18–37) to determine the optimum number of cycles for this analysis. Based on these results, we used 32 cycles in subsequent experiments. After amplification, PCR products were analysed on an ABI377 automated sequencer (Perkin Elmer) where they resolved into two major fragments (327 and 418 bp, exons 9–11; 487 and 578 bp, exon 9–13) corresponding to *tau* transcripts with and without exon 10. The identity of each band was confirmed by sequence analysis. The molar ratio of exon10$^+$ to exon 10$^-$ RNA was determined using Genescan software. Three independent PCRs (for both exons 9–11 and 9–13) were used to determine the mean and s.d. of the ratio for each brain. Results (not shown) were essentially identical when exon $10^{+/-}$ ratios were estimated by densitometric analysis of PCR products on agarose gels using a Kodak DC120 camera kit and ID Image Gel densitometry software.

Exon-trapping analysis of exon-10 splicing. Mutant and wild-type versions of *tau* exon 10 were amplified from the DNA of patients with each of the three different splice mutations (+13, +14 and +16) and from normal individuals. PCR products contained exon 10 and ~40 bp of flanking intron sequence at either end. PCR products were cloned into the splicing vector pSPL3b using *Xho*I and *Pst*I sites incorporated into the amplification products. Mutant and wild-type constructs were identified by sequence analysis. For exon trapping, the exon-trapping system of Life Technologies was used. Briefly, COS-7 cells were transfected in duplicate with 1 μg each construct using LipofectACE reagent (Life Technologies). Cells were collected 24 h post-transfection and RNA prepared using the Trizol reagent (Life Technologies). First-strand synthesis and nested PCR were done using reagents supplied with the system and conditions described in manufacturer's instructions, except that *Bst*X1 digestion of primary PCR products was excluded. To verify that the RT-PCR was quantitative, different amounts of primary PCR template (1–5 μl) were used and the total number of amplification cycles was varied (30–35 cycles). PCR products were analysed on 3% Metaphore (FMC) gels. RT-PCR products (Fig. 3) had their identities confirmed by sequencing.

Received 9 April; accepted 1 June 1998.

1. Foster, N. L. *et al.* Frontotemporal Dementia and Parkinsonism Linked to Chromosome 17: A Consensus Statement. *Annu. Neurol.* **41**, 706–715 (1997).
2. Wilhelmsen, K. C., Lynch, T., Pavlou, E. & Nygaard, T. G. Localization of disinhibition-dementia-parkinsonism-amyotrophy complex to 17q21-22. *Am. J. Hum. Genet.* **55**, 1159–1165 (1994).
3. Baker, M. *et al.* Localization of frontotemporal dementia with parkinsonism in an Australian kindred to chromosome 17q21-22. *Annu. Neurol.* **42**, 794–798 (1997).
4. Froelich, S. *et al.* Mapping of a disease loc. for familial rapidly progressive frontotemporal dementia to chromosome 17q12-21. *Am. J. Med. Genet.* **74**, 380–385 (1997).
5. Murrell, J. *et al.* Familial multiple system tauopathy with presenile dementia localized to chromosome 17. *Am. J. Hum. Genet.* **61**, 1131–1138 (1997).
6. Wijker, M. *et al.* Localization of the gene for rapidly progressive autosomal dominant parkinsonism and dementia with pallido-ponto-nigral degeneration to chromosome 17q21. *Hum. Mol. Genet.* **5**, 151–154 (1996).
7. Heutink, P. *et al.* Hereditary fronto-temporal dementia is linked to chromosome 17q21-22. A genetic and clinico-pathological study of three Dutch families. *Annu. Neurol.* **41**, 150–159 (1997).
8. Yamaoka, L. H. *et al.* Linkage of frontotemporal dementia to chromosome 17- clinical and neuropathological characterization of phenotype. *Am. J. Hum. Genet.* **59**, 1306–1312 (1996).
9. Dark, F. A family with autosomal dominant, non-Alzheimer's presenile dementia. *Austr. N. Z. J. Psychiat.* **31**, 139–144 (1997).
10. Constantinidis, J., Richard, J. & Tissot, R. Pick's disease: Histological and clinical classification. *Eur. Neurol.* **11**, 208–217 (1974).
11. Andreadis, A., Brown, W. M. & Kosik, K. S. Structure and novel exons of the human *tau* gene. *Biochemistry* **31**, 10626–10633 (1992).
12. Spillantini, M. G., Bird, T. D. & Ghetti, B. Frontotemporal dementia and parkinsonism linked to chromosome 17: A new group of tauopathies. *Brain Path.* **8**, 387–402 (1998).
13. Goedert, M., Spillantini, M. G., Potier, M. C., Ulrich, J. & Crowther, R. A. Cloning and sequencing of the cDNA encoding an isoform of microtubule-associated protein *tau* containing four tandem repeats: differential expression of tau protein mRNAs in human brain. *EMBO J.* **8**, 393–399 (1989).
14. Spillantini, M. G. *et al.* Familial multiple system tauopathy with presenile dementia: a disease with abundant neuronal and glial tau filaments. *Proc. Natl Acad. Sci. USA* **94**, 4113–4118 (1997).
15. Goedert, M. *et al.* Assembly of microtubule-associated protein *tau* into Alzheimer-like filaments induced by sulphated glycosaminoglycans. *Nature* **383**, 550–553 (1996).
16. Goedert, M., Spillantini, M. G., Jakes, R., Rutherford, D. & Crowther, R. A. Multiple isoforms of human microtubule-associated protein *tau*: sequence and localization in neurofibrillary tangles of Alzheimer's disease. *Neuron* **3**, 519–526 (1989).
17. The Lund and Manchester groups. Clinical and neuropathological criteria for frontotemporal dementia. *J. Neurol. Neurosurg. Psychiat.* **57**, 416–418 (1994).
18. Butner, K. A. Kirschner, M. W. J. *Tau* protein binds to microtubules through a flexible array of distributed weak sites. *J. Cell. Biol.* **115**, 717–730 (1991).
19. Reed, L. A. *et al.* Autosomal dominant dementia with widespread neurofibrillary tangles. *Annu. Neurol.* **42**, 564–572 (1997).
20. McGeer, P. L., Schwab, C., McGeer, E. G., Haddock, R. L. & Steele, J. C. Familial nature and continuing morbidity of the amyotropic lateral sclerosis-parkinsonism dementia complex of Guam. *Neurology* **49**, 400–409 (1997).
21. Goedert, M. Tau protein and the neurofibrillary pathology of Alzheimer's disease. *Trends Neurosci.* **16**, 460–465 (1993).
22. Church, D. M. *et al.* Isolation of genes from complex sources of mammalian genomic DNA using exon amplification. *Nature Genet* **6**, 98–105 (1994).
23. Eperon, L. P., Graham, I. R., Griffiths, A. D. & Eperon, I. C. Effects of RNA secondary structure on alternative splicing of pre-mRNA: is folding limited to a region behind the transcribing RNA polymerase? *Cell* **54**, 393–401 (1988).
24. Kuo, H.-C., Nasim, F.-U. H. & Grabowski, P. J. Control of alternative splicing by the differential binding of U1 small nuclear ribonucleoprotein particle. *Science* **1251**, 1045–1050 (1991).
25. Dickson, D. Neurodegenerative diseases with cytoskeletal pathology: a biochemical classification. *Annu. Neurol.* **42**, 541–543 (1997).
26. Conrad, C. *et al.* Genetic evidence of the involvement of τ in progressive supranuclear palsy. *Annu. Neurol.* **41**, 277–281 (1997).
27. Higgins, J. J., Litvan, I., Pho, L. T., Li, W. & Nee, L. E. Progressive supranuclear palsy is in linkage disequilibrium with the τ and not the α-synuclein gene. *Neurology* **50**, 270–273 (1998).
28. Freier, S. M. *et al.* Improved free-energy parameters for predictions of RNA duplex stability. *Proc. Natl Acad. Sci. USA* **83**, 9373–9377 (1986).

Acknowledgements. This work was supported by an NINDS (RO1) grant to MH, an NIA (MCSDA) grant to T.L. and NIA (P50) grants to A.G. and J.C.M. and to M.H., J.H. and R.C.P. Additional support was provided by the Mayo Foundation (M.H., J.H.), the International Foundation for Alzheimer Research, the Dutch Brain Research Foundation (P.H.) and Judith Mason (P. Dodd). A.G. is the recipient of an NIH career development award (NIA). C.L.L. was a Washington University Alzheimer's Disease Research Center postdoctoral fellow. P.R. is the recipient of a TMG of EU grant. J.M.K. is the recipient of an NSADA award. T.L. is the recipient of Irving Scholar, NARSAD and Parkins's Disease Foundation awards. We thank the Mayo Clinic Molecular Biology Core Facility for sequencing and acknowledge the support of the Dutch Brain Bank (W.K., R.R.), the Michigan ADRC Brain Bank and the Columbia University Brain Bank. The participation of the families has been crucial.

Correspondence and requests for materials should be addressed to M.H. (e-mail: hutton.michael@mayo.edu) or P.H. (e-mail: heutink@kgen.fgg.eur.nl).

The antigenic structure of the HIV gp120 envelope glycoprotein

Richard Wyatt*, Peter D. Kwong†, Elizabeth Desjardins*, Raymond W. Sweet‡, James Robinson§, Wayne A. Hendrickson† & Joseph G. Sodroski*‖

** Department of Cancer Immunology and AIDS, Dana-Farber Cancer Institute, Department of Pathology, Harvard Medical School, and ‖ Department of Immunology and Infectious Diseases, Harvard School of Public Health, Boston, Massachusetts 02115, USA*

† Department of Biochemistry and Molecular Biophysics, Howard Hughes Medical Institute, Columbia University, New York, New York 10032, USA

‡ SmithKline Beecham Pharmaceuticals, 709 Swedeland Road, King of Prussia, Pennsylvania 19406-0939, USA

§ Department of Pediatrics, Tulane University Medical Center, 1430 Tulane Avenue, New Orleans, Louisiana 70112, USA

The human immunodeficiency virus HIV-1 establishes persistent infections in humans which lead to acquired immunodeficiency syndrome (AIDS). The HIV-1 envelope glycoproteins, gp120 and gp41, are assembled into a trimeric complex that mediates virus entry into target cells[1]. HIV-1 entry depends on the sequential interaction of the gp120 exterior envelope glycoprotein with the receptors on the cell, CD4 and members of the chemokine receptor family[2–4]. The gp120 glycoprotein, which can be shed from the envelope complex, elicits both virus-neutralizing and non-neutralizing antibodies during natural infection. Antibodies that lack neutralizing activity are often directed against the gp120 regions that are occluded on the assembled trimer and which are exposed only upon shedding[5,6]. Neutralizing antibodies, by contrast, must access the functional envelope glycoprotein complex[7] and typically recognize conserved or variable epitopes near the receptor-binding regions[8–11]. Here we describe the spatial organization of conserved neutralization epitopes on gp120, using epitope

maps in conjunction with the X-ray crystal structure of a ternary complex that includes a gp120 core, CD4 and a neutralizing antibody[12]. A large fraction of the predicted accessible surface of gp120 in the trimer is composed of variable, heavily glycosylated core and loop structures that surround the receptor-binding regions. Understanding the structural basis for the ability of HIV-1 to evade the humoral immune response should assist in the design of a vaccine.

The amino-acid sequence of human and simian immunodeficiency virus gp120 glycoproteins consists of five variable regions (V1–V5) interposed among more conserved regions[13]. Variable regions V1–V4 form exposed loops anchored at their bases by disulphide bonds[14].

Neutralizing antibodies recognize both variable and conserved gp120 structures. The V2 and V3 loops contain epitopes for strain-restricted neutralizing antibodies[15–17]. More broadly neutralizing antibodies recognize discontinuous, conserved epitopes in three regions of the gp120 glycoprotein (Table 1). In HIV-1-infected humans, the most abundant of these are directed against the CD4-binding site (CD4BS) and block gp120–CD4 interaction[8,9]. Less common are antibodies against epitopes induced or exposed upon CD4 binding (CD4i)[18]. Both CD4i and V3 antibodies disrupt the binding of gp120–CD4 complexes to chemokine receptors[10,11]. A third gp120 neutralization epitope is defined by a unique monoclonal antibody, 2G12 (ref. 19), which does not efficiently block receptor binding[11].

In the accompanying Article[12], we report the X-ray crystal structure of an HIV-1 gp120 core in a ternary complex with two-domain soluble CD4 and the Fab fragment of the CD4i antibody 17b. The gp120 core lacks the V1/V2 and V3 variable loops, as well as amino- and carboxy-terminal sequences, which interact with the gp41 glycoprotein[6], and is enzymatically deglycosylated[12,20]. Despite these modifications, the gp120 core binds CD4 and antibodies against CD4BS and CD4i epitopes[20,21] and thus retains structural integrity. The gp120 core is composed of an inner domain, an outer domain and a third element, the 'bridging sheet'[12] (Fig. 1a). All three structural elements contribute, either directly or indirectly, to CD4 and chemokine-receptor binding [2]. We now analyse the organization of the surface of the gp120 core in light of the known antibody responses directed against this exposed viral glycoprotein.

Although generally well conserved compared with the five variable regions, some variability in the surface of the gp120 core is evident when the sequences of all primate immunodeficiency viruses are analysed. This variability is disproportionately associated with the surface of the outer domain proximal to the V4 and V5 regions and removed from the receptor-binding regions (Fig. 1a–c). The ℒA, ℒC, ℒD and ℒE surface loops[12] contribute to the variability of this surface. The potential *N*-linked glycosylation sites present in the gp120 core are concentrated in this variable half of the protein (Fig. 1b, c). The only conserved residues apparent on this relatively variable surface are asparagine 356 and threonine/serine 358, which constitute a complex carbohydrate addition site within the ℒE loop (Fig. 1b, c). As most carbohydrate moieties may appear as 'self' to the immune system, the extensive glycosylation of the outer domain surface may render it less visible to immune surveillance. This helps to explain why antibodies directed against this gp120 surface have been identified so infrequently.

The receptor-binding regions retained in the gp120 core are well conserved among primate immunodeficiency viruses[12]. Also highly conserved is the surface of the inner domain spanned by the α1 helix and located opposite the variable surface described above (Fig. 1d). This surface is likely to interact with gp41 and/or with N-terminal gp120 segments absent from the gp120 core. This inner domain surface and the receptor-binding regions are devoid of glycosylation.

In conjunction with prior mutagenic and antibody competition analyses[5,6,18–20,22] the gp120 core structure reveals the spatial positioning of the conserved gp120 neutralization epitopes. Although the principal variable loops are either absent (V1/V2 and V3) or poorly resolved (V4) in the gp120 core structure, their approximate positions can be deduced (Fig. 2a). The conserved gp120 neutralization epitopes are discussed in relation to these variable loops and the variable, glycosylated core surface.

CD4i epitopes. The gp120 epitope recognized by the CD4i antibody 17b can be directly visualized in the crystallized ternary complex[12] (Fig. 2b, c). Strands from the gp120 fourth conserved (C4) region and the V1/V2 stem contribute to an antiparallel β-sheet (the 'bridging sheet'; Fig. 1a) that contacts the antibody. Most gp120 residues previously implicated in the formation of the CD4i epitopes[18] (Table 1) are located either within this β-sheet or in nearby structures. With the exception of Thr 202 and Met 434, the gp120 residues in contact with the 17b Fab are highly conserved among HIV-1 isolates (Figs 1c, 2a). The prominent ('male') CDR3 loop of the 17b heavy chain dominates the contacts with gp120, with

Table 1 Conserved epitopes for neutralizing antibodies identified on the gp120 core

Competition group*	Examples of monoclonal antibodies	gp120 amino acids†	Probable mechanism of virus neutralization	Properties	Selected refs
CD4-binding site (CD4BS)	F105 15e 21h 1125h 448D 39.3 IgG1b12 830D	Asn 88 (13), Asp 113 (50), Lys 117 (25), Ser 256 (75), Thr 257 (75), Asn 262 (63), Ala 266 (13), Asp 368 (100), Glu 370 (100), Tyr 384 (13), Lys 421 (50), Trp 427 (25), Asp 457 (13), Pro 470 (25), Asp 474 (13), Met 475 (13), Asp 477 (63), Asp/Leu/ Tyr 482/483/484 (25)	Interference with gp120–CD4 binding	CD4BS antibodies compete with CD4 and with antibodies against CD4i epitopes	8, 9, 22
CD4-induced epitopes (CD4i)	17b 48d	Asn 88, Lys 117, Lys 121, Lys 207, Ser 256, Thr 257, Asn 262, ΔV3, Glu 370, Glu 381, Phe 382, Arg 419, Ile 420, Lys 421, Gln 422, Ile 423, Trp 427, Tyr 435, Pro 438, Met 475	Interference with chemokine-receptor binding	CD4 binding increases exposure of the epitopes as a result of movement of the V2 variable loop	18; C. Rizzuto and J.G.S., submitted
2G12	2G12	Asn 295, Thr 297, Ser 334, Asn 386, Asn 392, Asn 397	Unknown	Antibody binding is dependent upon proper *N*-linked glycosylation	19

* The gp120 competition groups are defined as in ref. 5.
† The gp120 amino acids are numbered according to the sequence of the HXBc2 (IIIB) gp120 glycoprotein, where residue 1 is the methionine at the amino terminus of the signal peptide. Changes in the amino acids listed resulted in significant reduction in antibody binding to the gp120 glycoprotein (refs 18, 19, 22). Numbers in parentheses indicate the percentage of CD4BS antibodies examined whose binding is decreased by changes in the indicated residue.

additional contacts through the heavy chain CDR2 (ref. 12). Unusually, there are minimal 17b light-chain contacts, leaving a large gap between the gp120 co.e and most of the 17b light-chain surface. In the complete gp120 glycoprotein, this gap is probably occupied by the V3 loop. This is consistent with the position and orientation of the V3 base on the gp120 core structure[12], the effect of V3 deletions on the binding of CD4i antibodies in the absence of soluble CD4 (ref. 21), the competition of some V3-directed antibodies with CD4i antibodies[5], and the ability of both antibody groups to block chemokine-receptor binding[10,11]. The chemokine-receptor-binding region of gp120 probably consists of elements near or within the 'bridging sheet' and the V3 loop (Fig. 1a), a model that is supported by recent mutagenic analysis (C. Rizzuto *et al.*, submitted).

The V2 loop probably resides on the side of the 17b epitope opposite the V3 loop (Fig. 2a). The V1/V2 loops, which vary from 57 to 86 residues in length[13], are dispensable for HIV-1 replication[21,23], but decrease the sensitivity of viruses to neutraliza-

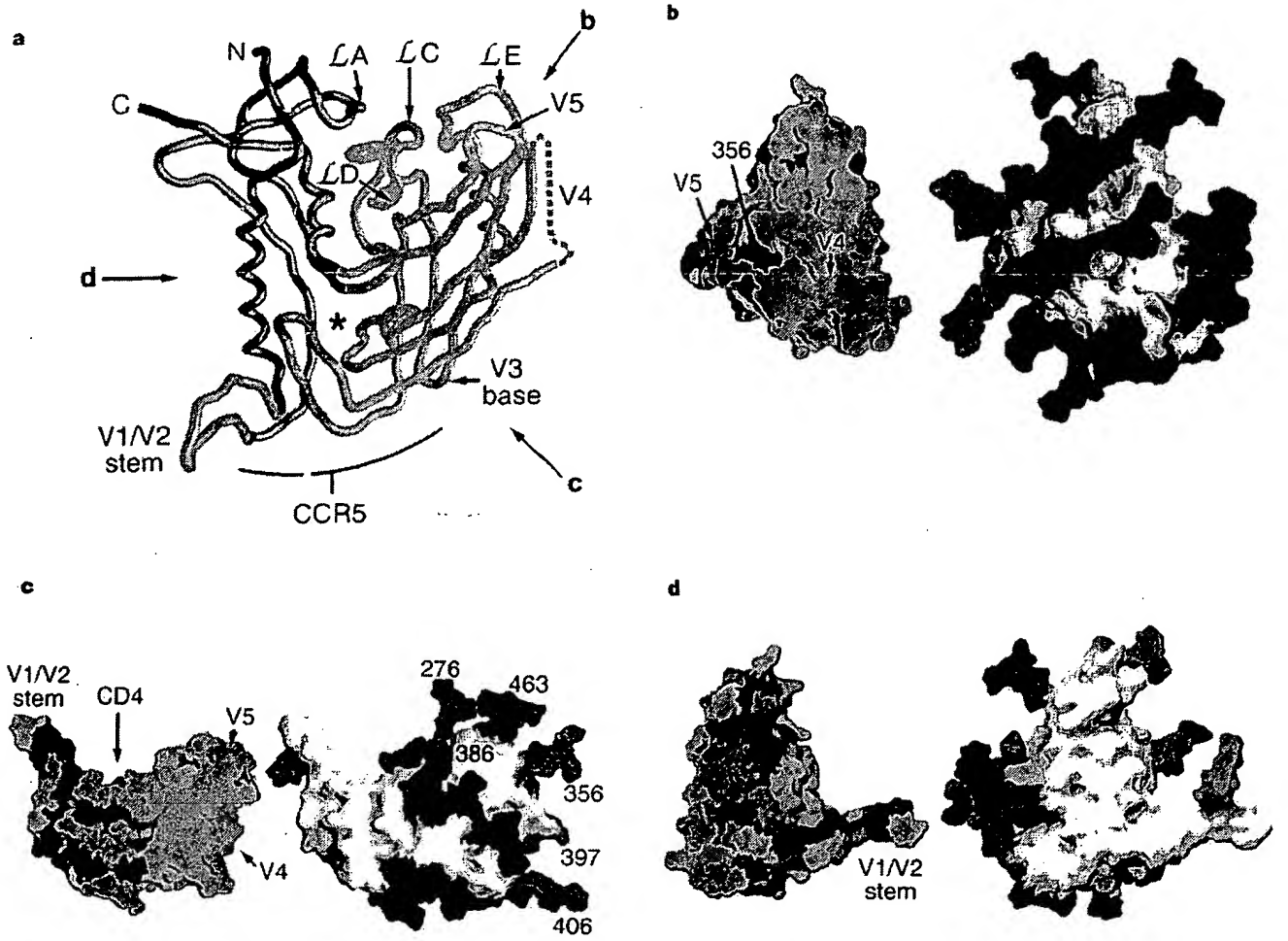

Figure 1 Structure and orientation of the HIV-1 gp120 core. **a**, A Cα tracing of the gp120 core, which was crystallized in a ternary complex with two-domain soluble CD4 and the Fab fragment of the 17b antibody[12], is shown. The gp120 core is seen from the perspective of CD4, and is oriented with the viral membrane at the top of the figure and the target cell membrane at the bottom. The inner gp120 domain is shown in red and the outer domain in yellow; the 'bridging sheet' is orange. The N and C termini of the truncated gp120 core are labelled, as are the positions of structures related to the gp120 variable regions V1-V5. The ℒA, ℒC, ℒD and ℒE surface loops[12] are shown. The position of the Phe 43 cavity involved in CD4 binding is indicated by an asterisk. The gp120 surface implicated in binding to the CCR5 chemokine receptor (C. Rizzuto and J.G.S., submitted) is shown. The perspectives shown in **b**–**d** are indicated. **b**, View of the molecular surface of the gp120 outer domain, from the perspective indicated in **a**. The molecular surface on the left is coloured according to the variability observed in gp120 residues among primate immunodeficiency viruses: red, residues conserved among all primate immunodeficiency viruses; orange, residues conserved in all HIV-1 isolates; yellow, residues exhibiting some variation among HIV-1 isolates; and green, residues showing significant variability among HIV-1 isolates (see Methods). The variability of the gp120 surface is underestimated here because the V4 variable loop, which is not resolved in the structure, contributes to this surface (approximate location is indicated). The position of the V5 region is shown. Also note the highly conserved glycosylation site (Asn 356 and Thr/Ser 358) within the ℒE loop, between the V5 and V4 regions. On the right, the V4 loop and the carbohydrates are modelled (see Methods). The complex carbohydrate addition sites used in mammalian cells[14] are coloured light blue, and the high-mannose sites are dark blue. The gp120 protein surface is in white. **c**, View of the gp120 molecular surface that faces the target cell. Variability is indicated on the left, using the same colour scheme as in **b**. Note the clear demarcation between the conserved surface, which has been implicated in the formation of CD4i epitopes[18] and in chemokine-receptor binding (C. Rizzuto and J.G.S., submitted), and the variable surface of the outer domain. The recessed binding site for CD4 is indicated, flanked by the V1/V2 stem, which is labelled. The V4 loop and the carbohydrates are modelled on the right (colouring as in **b**). Particular carbohydrates referred to in the text are labelled. **d**, View of the molecular surface of the gp120 core inner domain. Variability is indicated on the left by the colour scheme used in **b**. The CD4-binding site is on the right; the protruding V1/V2 stem is indicated. The conserved molecular surface, which is associated with the inner domain of the gp120 core, is devoid of known *N*-linked glycosylation sites. These are modelled on the right, which is coloured as in **b**.

tion by antibodies against V3 and CD4i epitopes[23]. The latter effect is mediated primarily by the V2 loop[21], suggesting that part of the V2 loop folds back along the V1/V2 stem to mask the 'bridging sheet' and adjacent V3 loop. The proximity of the V2 and V3 loops is supported by the observation that, in monkeys infected with simian–human immunodeficiency viruses (SHIVs), neutralizing antibodies are raised against discontinuous epitopes with V2 and V3 components (B. Etemad-Moghadam *et al.*, submitted). The CD4i epitopes are probably masked by the flanking V2 and V3 loops, requiring the evolution of antibodies with protruding ('male') complementarity-determining regions (CDRs) to access these conserved epitopes. It has been suggested that CD4 binding repositions the V1/V2 loops, thus exposing the CD4i epitopes[21]. The presence of contacts between the V1/V2 stem and CD4 in the crystal structure[12] is consistent with this model.

CD4BS epitopes. CD4 makes several contacts within a recessed pocket on the gp120 surface. The gp120–CD4 interface includes two cavities, one water-filled and bounded equally by both proteins,

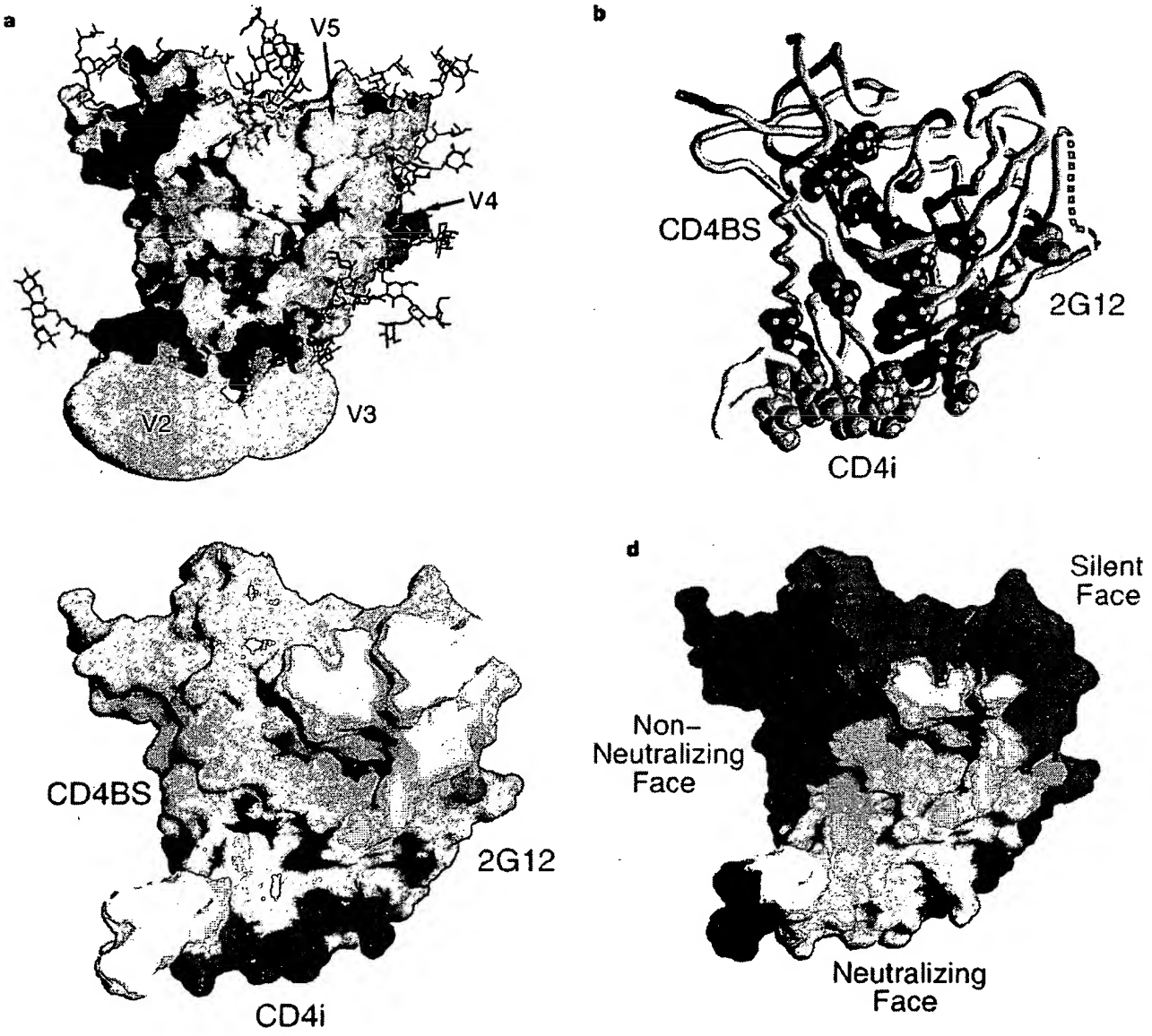

Figure 2 The spatial relationship of epitopes on the HIV-1 gp120 glycoprotein. **a**, The molecular surface of the gp120 core is shown, using the same perspective as in Fig. 1a. The modelled N-terminal gp120 core residues, V4 loop and carbohydrate structures are included. The variability of the molecular surface is indicated (colour scheme as in Fig. 1b). The modelled carbohydrates are shown in light blue (complex sugars) or dark blue (high-mannose sugars). The approximate locations of the V2 and V3 variable loops are indicated. Note the well-conserved surfaces near the 'Phe 43' cavity and the chemokine-receptor-binding site (Fig. 1a). **b**, Cα tracing of the gp120 core, oriented as in Fig. 1a. The gp120 residues within 4 Å of the 17b CD4i antibody are shown in green; those implicated in the binding of CD4BS antibodies[22] are in red. Changes in these residues significantly affect the binding of at least 25% of the CD4BS antibodies listed in Table 1. The residues implicated in 2G12 binding[19] are shown in blue. The V4 variable loop, which contributes to the 2G12 epitope[19], is indicated by dotted lines. **c**, The molecular surface of the gp120 core, oriented and coloured as in **b**. **d**, Approximate locations of the faces of the gp120 core, defined by the interaction of gp120 and antibodies. The molecular surface accessible to neutralizing ligands (CD4 and CD4BS, CD4i and 2G12 antibodies) is shown in white. The neutralizing face of the complete gp120 glycoprotein includes the V2 and V3 loops, which are found adjacent to the surface shown (**a**). The approximate location of the gp120 face that is poorly accessible on the assembled envelope glycoprotein trimer and therefore elicits only non-neutralizing antibodies[5,6] is shown in magenta. The approximate location of an immunologically 'silent' face of gp120, which roughly corresponds to the highly glycosylated outer domain surface, is in blue.

the other extending into the gp120 interior and contacting CD4 only at Phe 43 (Fig. 1a)[12]. Table 1 and Fig. 2b, c show the gp120 residues implicated in the formation of CD4BS epitopes recognized by eight representative antibodies. CD4BS epitopes are uniformly disrupted by changes in Asp 368 and Glu 370 (ref. 22), which surround the opening of the 'Phe 43 cavity'. These residues are located on a ridge at the intersection of the two receptor-binding gp120 surfaces, consistent with competition studies suggesting that CD4BS epitopes overlap both the CD4i epitopes and the binding site for CD4 (refs 5, 18). The location of the gp120 residues implicated in formation of the CD4BS epitopes suggests that important elements of the CD4-binding surface of gp120 are accessible to antibodies.

Some CD4BS antibodies, like IgG1b12, are particularly potent at neutralizing HIV-1 (ref. 24). IgG1b12 binding is disrupted by gp120 changes that affect the binding of other CD4BS antibodies but, atypically, is sensitive to changes in the V1/V2 stem–loop structure[25]. The observation that some well-conserved residues in the gp120 V1/V2 stem contact CD4 (ref. 12) raises the possibility that this protruding structure also contributes to the IgG1b12 epitope. This might increase the ability of the antibody to access the assembled envelope glycoprotein trimer, thus increasing neutralizing capability.

Although the CD4BS epitopes and the CD4-binding site overlap, several observations demonstrate that the binding of CD4BS antibodies differs from that of CD4. Changes in Trp 427, a gp120 residue that contacts both the Phe 43 cavity and CD4, uniformly disrupt CD4 binding but affect the binding of only some CD4BS antibodies (Table 1). Conversely, some changes in other cavity-lining gp120 residues, Ser 256 and Thr 257, affect the binding of CD4BS antibodies more than the binding of CD4 (ref. 22). As the recessed position of Ser 256 and Thr 257 in the current crystal structure (Fig. 2b, c) makes direct contacts with antibody unlikely, either the effects of changes in these residues are indirect or the CD4BS antibodies recognize a gp120 conformation that differs from the CD4-bound state. With respect to the latter possibility, it is interesting that several of the residues implicated in the integrity of the CD4BS epitopes are located in the interface between the inner and outer gp120 domains. CD4BS antibodies might recognize a gp120 conformation in which the spatial relationship between the domains is altered compared with the CD4-bound state, thus allowing better surface exposure of these residues. Differences between the CD4BS epitopes and the CD4-binding site create opportunities for neutralization escape[22]. The gp120 residues surrounding the Phe 43 cavity are highly conserved among primate immunodeficiency viruses (Fig. 2a), but the observed modest variation in adjacent surface-accessible residues (for example, Pro 369, Thr 373 and Lys 432) could account for decreased recognition of the gp120 glycoprotein from some geographic clades of HIV-1 by CD4BS antibodies[25]. Additional potential for variation near or within the CD4BS epitopes is created by the unusual water-filled cavity in the gp120–CD4 binding interface, because CD4 binding can apparently tolerate change in the gp120 residues contacting this cavity[12].

The recessed nature of the CD4-binding pocket on gp120 (Fig. 1c) may delay the generation of high-affinity antibodies against the CD4BS epitopes and may afford opportunities to minimize the antiviral efficacy of such antibodies once they are elicited. The degree of recession is probably much greater on the full-length glycosylated gp120 than is evident on the crystallized gp120 core. The recessed pocket is flanked on one side by the V1/V2 stem–loop structure. The characterization of HIV-1 escape mutants from the IgG1b12 CD4BS antibody and the mapping of several V2 conformational epitopes support a model in which the V2 loop folds back along the V1/V2 stem, with V2 residues 183–188 proximal to Asp 368 and Glu 370. This model is consistent with observations that V1/V2 changes, in combination with V3 changes, can alter the exposure of the adjacent CD4BS epitopes, particularly on the assembled trimer[26]. The high temperature factors associated with the V1/V2 stem[12] imply flexibility in this protruding element (Fig. 1c, d), expanding the potential range of space occupied by the V1/V2 stem–loop structure. This could increase masking of the adjacent CD4BS and CD4i gp120 epitopes and divert antibody responses towards the variable loops.

Glycosylation may modify the interaction of antibodies with CD4BS epitopes. The ℒD loop, on the rim of the CD4-binding pocket opposite the V1/V2 stem, contains a well-conserved glycosylation site, Asn 276 (Fig. 1c). Changes in this site and at the adjacent Ala 281 have been associated with escape from the neutralizing activity of patient sera[27] and have been seen in SHIVs extensively passaged in monkeys[28]. Another conserved glycosylation site at Asn 386 lies adjacent to both CD4BS and CD4i epitopes (Fig. 1c) and could diminish antibody responses against those sites. Additionally, in various HIV-1 strains, carbohydrates are added to the V2 loop segment (residues 186–188) thought to be proximal to the CD4BS epitopes.

The 2G12 epitope. The integrity of the 2G12 epitope is disrupted by changes in gp120 glycosylation, by either glycosidase treatment or mutagenic alteration of specific *N*-linked carbohydrate-addition sites[19]. These sites are located on the relatively variable surface of the gp120 outer domain, opposite to and approximately 25 Å away from the CD4-binding site (Fig. 2b, c). The gp120 glycoprotein synthesized in mammalian cells exhibits a dense concentration of high-mannose sugars in this region (Fig. 2a). Even in the enzymatically deglycosylated gp120 core, carbohydrate residues constitute much of this surface. 2G12 probably binds at least in part to these

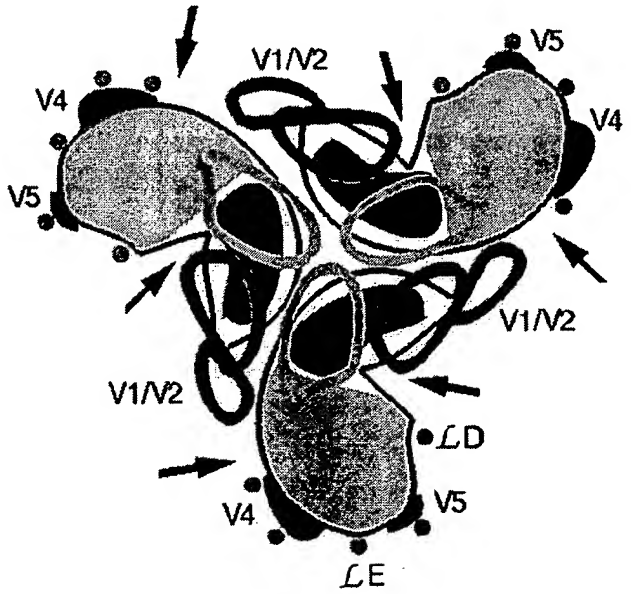

Figure 3 A likely arrangement of the HIV-1 gp120 glycoproteins in a trimeric complex. The gp120 core was organized into a trimeric array, based on the criteria discussed in the text. The perspective is from the target-cell membrane, like that in Fig. 1c. The CD4-binding pockets are indicated by black arrows, and the conserved chemokine-receptor-binding regions are in red. Areas shaded in light green indicate the more variable, glycosylated surfaces of the gp120 cores. The approximate locations of the 2G12 epitopes are indicated by blue arrows; those of the V3 loops (yellow) and V4 regions (green) are indicated. The positions of the V5 regions (green) and some complex-carbohydrate addition sites (asparagines 276, 463, 356, 397 and 406) (blue dots) are shown. The approximate locations of the large V1/V2 loops, centred on the known positions of the V1/V2 stems, are indicated (green). On one of the gp120 subunits, the positions of the ℒD and ℒE loops are indicated. The distance of each of the gp120 monomers from the 3-fold symmetry axis is arbitrary.

THE JOURNAL OF BIOLOGICAL CHEMISTRY
© 1996 by The American Society for Biochemistry and Molecular Biology, Inc.

Vol. 271, No. 23, Issue of June 7, pp. 13829–13833, 1996
Printed in U.S.A.

Contribution of Arginine Residues in the RP135 Peptide Derived from the V3 Loop of gp120 to Its Interaction with the Fv Fragment of the 0.5β HIV-1 Neutralizing Antibody*

(Received for publication, January 19, 1996, and in revised form, March 8, 1996)

Gabriel A. Faiman, Rina Levy, Jacob Anglister, and Amnon Horovitz‡

From the Department of Structural Biology, Weizmann Institute of Science, Rehovot 76100, Israel

The construction, expression, and purification of an active Fv fragment of the 0.5β monoclonal human immunodeficiency virus type 1 (HIV-1) neutralizing antibody is reported. The interaction between the Fv fragment and the RP135 peptide derived from the V3 loop of gp120 from HIV-1_{IIIB} was studied by varying the salt concentration and by mutating arginine residues in the peptide. The mutations R4A, R8A and R11A (which correspond to residues 311, 315, and 318 in gp120 of HIV-1_{IIIB}) reduce the binding free energy by 0.22 (± 0.20), 4.32 (± 0.16), and 1.58 (± 0.17) kca mol^{-1}, respectively. The salt-dependent components of their contributions to binding are 0.02 (± 0.22), −0.55 (± 0.18), and −0.97 (± 0.19) kcal mol^{-1}, respectively. The magnitudes of the mutational effects and the extent of shielding by 1 M NaCl suggest that Arg-8 is involved in a buried salt bridge in the peptide-Fv fragment complex, whereas Arg-11 is involved in a more solvent-exposed electrostatic interaction.

The 0.5β monoclonal antibody was raised (1) against the envelope glycoprotein gp120 (from the strain HIV-1_{IIIB})[1] which is found on the surface of human immunodeficiency virus type 1 (HIV-1) and HIV-1-infected cells. Infection of healthy T-cells is facilitated by the binding of gp120 to the CD4 protein which is present on the surface of helper T-cells. A chimeric monoclonal antibody which contains the variable region of the 0.5β antibody and human constant regions was found to protect chimpanzees from HIV-1 infection after passive immunization (2). The 0.5β antibody binds to a sequential epitope of gp120 which corresponds to its principal neutralizing determinant. This determinant is within a disulfide-bridged loop in the third hypervariable region (V3) of gp120 (3, 4). A 24-amino acid-long peptide, NNTRKSIRIQRGPGRAFVTIGKIG, derived from the principal neutralizing determinant of gp120 of HIV-1_{IIIB} and designated RP135, is immunogenic by itself and was shown to correspond to the binding site of gp120 to the 0.5β antibody (4). Nuclear magnetic resonance (NMR) studies on the interaction of the RP135 peptide with the Fab fragment of the 0.5β antibody have defined a 16-residue epitope from Lys-5 to Ile-20 (5). The recently solved crystal structure of the Fab fragment of a different HIV-1 neutralizing antibody, 50.1, in complex with a 16-residue peptide derived from the V3 loop of gp120 (HIV-1_{MN} strain) shows that it interacts only with a sequential 7-residue epitope (6). The interaction between the Fab fragment of yet another HIV-1 neutralizing antibody, 59.1, with a 24-residue peptide is similar to that of the 50.1 Fab fragment with respect to the conformation of overlapping residues in the two peptides and the size of the epitope (7).

Recent advances in antibody technology (see, for review, Ref. 8) have made possible direct cloning of antibody genes from hybridomas or lymphocytes into plasmid vectors and their expression in bacteria (see, for review, Ref. 9). In particular, there has been much recent interest in smaller antibody fragments that still retain antigen binding activity. These include Fv fragments (10, 11), single-chain Fv fragments (12, 13) and Fab fragments (14). Owing to the relatively small size of Fv and single-chain Fv fragments, their structures can be determined by multidimensional NMR techniques (15), and they are expected to have improved pharmacokinetic properties (8). A single-chain Fv of the anti-HIV-1 gp120 antibody, F105, has been constructed previously (16). Here, we report the construction, expression, and purification of an active Fv fragment of the 0.5β monoclonal HIV-1 neutralizing antibody (1, 17). An accurate assay for measuring the binding of the RP135 peptide to the 0.5β Fv fragment was established and used to determine the contributions to binding of arginine residues in the peptide and their salt dependence. We have focused on arginine residues in the peptide since amino acid sequence information and model building (5) suggested that electrostatic interactions are of special importance in this system. Measurement of binding constants in the presence of high salt, which masks electrostatic interactions, facilitates partitioning of the binding energy into ionic and nonionic components. Our long-term goal is to analyze in detail the energetics of this interaction by kinetic and protein engineering methods and to determine the solution and crystal structures of the 0.5β Fv fragment-RP135 peptide complex.

EXPERIMENTAL PROCEDURES

Materials—Molecular biology reagents were from New England Biolabs or Promega unless stated otherwise. All Fmoc amino acid derivatives used for peptide synthesis were purchased from Novabiochem, Switzerland. Molecular weight prestained markers were from Bio-Rad. Isopropyl-1-thio-β-D-galactopyranoside (IPTG) was obtained from Chembridge Corp. All other analytical grade reagents were purchased from Sigma.

Cloning of Amplified DNA and Construction of the 0.5β Fv Fragment Expression Vector—The 54′CB1 hybridoma cell line producing the 0.5β monoclonal antibody was provided by Dr. S. Matsushita (Kumamoto University). Total RNA of 54′CB1 cells was purified using an Amer-

* This work was supported by Grant 91-00288 from the United States-Israel Binational Science Foundation (BSF), Jerusalem, Israel (to A. H.) and by a grant of the Israel Science Foundation administered by the Israel Academy of Sciences and Humanities (to J. A.). The costs of publication of this article were defrayed in part by the payment of page charges. This article must therefore be hereby marked "*advertisement*" in accordance with 18 U.S.C. Section 1734 solely to indicate this fact.

‡ Incumbent of the Robert Edward and Roselyn Rich Manson Career Development Chair. To whom correspondence should be addressed. Tel.: 972-8-934-3399; Fax: 972-8-934-4188; E-mail: csamnon@weizmann.weizmann.ac.il.

[1] The abbreviations used are: HIV, human immunodeficiency virus; Fmoc, *N*-(9-fluorenyl)methoxycarbonyl; IPTG, isopropyl-1-thio-β-D-galactopyranoside; PCR, polymerase chain reaction; HPLC, high performance liquid chromatography.

sham kit. The design of the PCR primers and the PCR amplification reactions were as before (18). The amplified PCR products were digested using *Pst*I and *Bst*EII for the V_H gene and *Sac*I and *Bgl*II for the V_κ gene. The digested PCR products were then subcloned into a pUC19 expression vector that previously contained the genes of the V_H and V_κ domains of the D1.3 anti-lysozyme antibody, each fused to the pelB signal sequence. In this plasmid, generously donated to us by Dr. G. Winter (Medical Research Council, Cambridge), the V_κ domain is fused at its C terminus to the *myc* tag peptide. The D1.3 pUC19 vector was digested with *Pst*I and *Bst*EII, purified to remove the DNA coding for the V_H domain of the D1.3 antibody, and then religated with the PCR product of the 0.5β antibody V_H gene. The product of this ligation reaction was then digested with *Sac*I and *Xho*I, purified to remove the DNA coding for the D1.3 V_κ domain, and then religated with the PCR product of the 0.5β antibody V_κ gene. A 0.9-kb *Eco*RI-*Hin*dIII restriction fragment of this plasmid was then subcloned into the pTZ19U vector (19) previously digested with the same enzymes. This vector is designated pTβ. The pTZ19U vector contains an f1 origin of replication that allows production of single-stranded DNA upon infection with helper phage.

Site-directed Mutagenesis—Single-stranded DNA of the plasmid pTβ, harbored in the *E. coli* strain TG2, was obtained by infecting these cells with helper-phage M13KO7 (Pharmacia Biotech Inc.). Site-directed mutagenesis was carried out using the method of Eckstein (20) and the Amersham kit. The following oligonucleotides were used to correct mutations owing to the PCR oligonucleotides (18) and to reverse an additional mutation Ser-25 → Phe that occurred for reasons not known. Glu-6(H) → Gln: 5′-CCCCAGACTG*CTGCAGCT-3′, Thr-114(H) → Ser: 5′-CGGTGACCGA*GGTCCCTT-3′, Phe-25(H) → Ser: 5′-GTGTAGCCAG*AAGCCTTGC-3′, Glu-3(κ) → Val: 5′-GGGTGAGCA*CGATGTC-3′, where H and κ indicate mutations in the heavy and light chains, respectively. An asterisk follows the mismatched bases. The *myc* tag peptide was removed by replacing the sequence coding for the first two N-terminal residues of the tag with stop codons using the oligonucleotide: 5′-CTGAGATGAGTTTTTGTTA*T*T*A*TTTGATCTCGAGCTTGG-3′. The vector with these five changes is designated pTβ11.

Fv Fragment Expression and Purification—A 5-ml starter culture of *Escherichia coli* TG2 cells harboring the pTβ11 plasmid was grown overnight at 37 °C in 2 × TY medium containing 50 μg/ml ampicillin and 0.1% glucose. This culture was used to inoculate 500 ml of 2 × TY medium containing 50 μg/ml ampicillin and 0.1% glucose. The cells were grown until their density reached A_{600} = 0.6, and then protein expression was induced by the addition of 1 mM IPTG. The cells were grown for another 4 h at 30 °C, centrifuged, the supernatant (fraction A) was discarded, and the pellet was resuspended in 30 mM Tris-HCl buffer (pH 8.0) containing 20% sucrose, 1 mM EDTA, 0.6 mM phenylmethylsulfonyl fluoride, 1 μg/ml aprotinin, and 1 μg/ml leupeptin. After incubation for 20 min at room temperature, the cells were spun and the supernatant was collected (fraction B). The cell pellets were resuspended in ice-cold water containing 0.5 mM $MgCl_2$, 0.6 mM phenylmethylsulfonyl fluoride, 1 μg/ml aprotinin, and 1 μg/ml leupeptin and incubated for 5 min on ice. After spinning the cells, the supernatant (fraction C) was collected and combined with fraction B. The combined fractions were loaded onto a Sepharose 4B (Pharmacia) column followed by an affinity column prepared by cross-linking a RP135-related peptide to CNBr-activated Sepharose 4B (Pharmacia), as described by the manufacturer. After extensive washing with PBS and 3 M NaCl, the 0.5β Fv fragment was eluted with 0.1 M phosphate-citrate buffer (pH 4.5), and 1-ml fractions were collected in tubes containing 50 μl of 3 M Tris-HCl (pH 9.0). The fractions were pooled, concentrated using Centriprep-10 (Amicon), and dialyzed exhaustively against 50 mM phosphate buffer (pH 7.5). The protein was then aliquoted, flash-frozen in liquid nitrogen, and stored at −70 °C. The concentration of the protein was determined using the method of Gill and von Hippel (21) and by quantitative amino acid analysis.

Peptide Synthesis and Purification—The antigenic peptide TRKSIRIQRGPGRAFVTIGK and variants thereof were synthesized by the solid-phase method using a multiple peptide synthesizer (AMS 422 Abimed Analysen-Technik GmbH, Germany). α-Amino functional groups were protected by Fmoc. Side-chain protecting groups were as follows: arginine, N^g-2,2,5,7,8-pentamethylchroman-6-sulfonyl (Pmc); serine, *O*-*t*-butyl; lysine, N^κ-*t*-butyloxycarbonyl; glutamine, N^γ-trityl. After the full chain was synthesized, the peptides were cleaved from the polymer using a mixture of trifluoroacetic acid, thioanisole and triethylsilane (9, 0.5, 0.5; v/v, respectively) at room temperature for 2 h. The cleaved peptides were precipitated with ice-cold *t*-butyl methyl ether and collected by centrifugation (4 °C, 2000 rpm). Pellets were twice washed with ether and then centrifuged. The pellets were then dissolved in double-distilled water and lyophilized. Crude peptides were purified by preparative HPLC on a RP-18 column (7 μm, Merck). Peptides were eluted from the RP-18 column with a linear acetonitrile gradient from 5 to 65% (v/v) in water with 0.01% trifluoroacetic acid at a flow rate of 4 ml/min. The molecular weights of the peptides were determined using a VG Platform mass spectrometer equipped with an electrospray ion source. 50 pmol/μl solutions of the peptides were analyzed by direct injection after calibration with myoglobin. The expected (E) and observed (O) molecular masses (in daltons) were found to be in excellent agreement (wild-type: 2240 (E), 2240.06 ± 0.8 (O); R4A: 2155 (E), 2154.91 ± 0.24 (O); R8A: 2155 (E), 2154.49 ± 0.34 (O); R11A: 2155 (E), 2154.62 ± 0.56 (O)). Species with other molecular masses were not detected except for trace amounts of the monosodium salt of the peptides. The compositions of the HPLC-pure peptides were verified by quantitative amino acid analysis using a Dionex amino acid analyzer. The concentrations of the peptides were estimated using the 2,4,6-trinitrobenzenesulfonic acid method for determination of amines (22).

Fluorescence Titration—A Shimadzu RF-540 spectrofluorimeter was used for all measurements. The excitation wavelength was 280 nm with a band pass of 10 nm and the emission wavelength was 330 nm with a band pass of 30 nm. A frozen aliquot of Fv was thawed and incubated for 30 min at 25.0 (± 0.1) °C with 2 ml of 50 mM phosphate buffer (pH 7.5) containing 0.05% Tween 20 and 1 M NaCl (when appropriate) before starting the titrations. The titrations were carried out by adding with a Hamilton syringe 2-μl samples of the peptide to the 0.5β Fv fragment of the antibody, with constant stirring in a thermostatted cuvette at 25.0 (± 0.1) °C. Fluorescence measurements were made 4 min after adding the peptide sample.

Data Analysis—Determination of dissociation constants was achieved by directly fitting fluorescence measurements of the Fv fragment at different peptide concentrations, using Kaleidagraph (version 2.1 Synergy Software (PCS Inc.)), to the following equation for tight binding:

$$F = F_0 + (F_\infty - F_0)([Fv]_T + [P]_T + K - ([Fv]_T + [P]_T + K)^2 - 4[Fv]_T[P]_T)^{1/2})/2[Fv]_T \quad \text{(Eq. 1)}$$

where F is the observed fluorescence, F_0 is the fluorescence in the absence of peptide, F_∞ is the fluorescence in the presence of saturating concentrations of peptide, $[Fv]_T$ and $[P]_T$ are the total Fv and peptide concentrations, and K is the dissociation constant. Estimates (±S.E.) of the parameters F_∞, $[Fv]_T$, and K were obtained from the fits which were carried out using a fixed value of F_0. In the case of weak binding, Equation 1 is reduced to:

$$F = (F_0 + F_\infty[P]/K)/(1 + [P]/K) \quad \text{(Eq. 2)}$$

where [P] is the concentration of free peptide and all other notations are as before. Determination of dissociation constants in the case of weak binding was achieved by directly fitting fluorescence measurements at different peptide concentrations to Equation 1 using a fixed value for $[Fv]_T$. Identical estimates were obtained by fitting the data to Equation 2. Standard free energies of binding were calculated from dissociation constants, as follows:

$$\Delta G = RT \ln K \quad \text{(Eq. 3)}$$

where R is the gas constant and T is the absolute temperature. The coupling energies between the effects on binding of the mutations and the addition of salt were calculated, as follows:

$$\Delta G_{int} = \Delta G(\text{wt, 0 M NaCl}) - \Delta G(\text{wt, 1 M NaCl}) - \Delta G(\text{mut, 0 M NaCl}) + \Delta G(\text{mut, 1 M NaCl}) \quad \text{(Eq. 4)}$$

The free energies on the right-hand side of Equation 4 are for binding of wild-type or mutant peptide to the 0.5β Fv fragment in the presence of 0 M or 1 M NaCl, as indicated.

RESULTS

Purification of the 0.5β Fv Fragment—In our pTβ11 plasmid construct, both the heavy and light chains of the 0.5β Fv fragment are fused to the pelB leader sequence and are, therefore, secreted into the periplasmic space. The 0.5β Fv was purified from the periplasmic space by osmotic shock. It may be seen in Fig. 1 that most of the purified 0.5β Fv was released from the cells upon addition of the sucrose buffer and before the

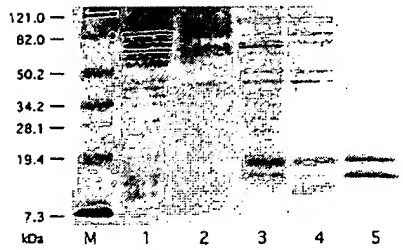

FIG. 1. **Analysis by SDS-polyacrylamide gel electrophoresis of steps in the purification of the 0.5β Fv antibody fragment.** In *lane 1* is shown total protein of IPTG-induced *E. coli* TG2 cells harboring the pTβ11 plasmid. Samples from fractions A, B, and C of the purification procedure and of the purified Fv are shown in *lanes 2–5*, respectively. *M* indicates molecular mass markers (kDa). 15% SDS-polyacrylamide gel electrophoresis was carried as described by Laemmli (31).

osmotic shock. The 0.5β Fv fragment was purified to homogeneity by affinity chromatography using a Sepharose 4B column to which a gp120-derived peptide antigen had been cross-linked. The final yield of the purified 0.5β Fv fragment is typically about 1 mg/liter using the expression and purification procedure described here. Correct processing and purification were confirmed by gel electrophoresis and amino acid analysis. The purified Fv fragment is stable as judged by two different assays. A linear relationship was observed between the activity of the Fv fragment and its concentration indicating that dissociation of the heavy and light chains is minimal (data not shown). In addition, repeated freeze and thaw cycles of the Fv fragment did not cause denaturation or dissociation as judged by nondenaturing gel electrophoresis (not shown).

Fluorescence Emission Spectra of the 0.5β Fv Fragment and Its Complex with the Peptide Antigen—Fluorescence emission spectra of the 0.5β Fv fragment were measured in the absence and in the presence of an excess amount of the RP135 peptide antigen (Fig. 2). As is evident from the spectra in Fig. 2, in the presence of excess antigen there is a blue-shift in λ_{max} from 337 nm to 333 nm, and there is an enhancement in the fluorescence intensity at wavelengths below 349 nm and quenching above this wavelength. These changes in fluorescence were exploited in order to establish a binding assay for the peptide antigen to the Fv fragment, as described under "Experimental Procedures." Previous model building (5) showed that the framework residue Trp-47(H) is part of the potential antigen-binding site. The observed changes in fluorescence may be due to this antibody residue which may be in contact with the peptide.

Effects of Mutations in the Peptide on Binding—Arginine residues at positions 4, 8, and 11 in the RP135 peptide, which correspond to positions 2, 6, and 9 in the peptides we synthesized and to positions 311, 315, and 318 in gp120, were replaced by alanine. The dissociation constants for the interaction of these peptides with the 0.5β Fv fragment were determined by fluorescence enhancement titration as shown in Fig. 3. Free energies of binding were calculated from the measured dissociation constants using Equation 3 (Table I). In the absence of salt, the dissociation constant for the interaction between wild-type peptide and the Fv fragment is about 2 nM. Skinner *et al.* (23) reported dissociation constants of 5 nM and 14 nM at 20 °C for the interaction of the full 0.5β antibody with gp120 and the RP135 peptide, respectively. The free energy of binding of the wild-type peptide to the Fv fragment is, in the absence of salt, −11.91 (± 0.16) kcal mol^{-1}. The mutations R4A, R8A, and R11A reduce the binding free energy by 0.22 (± 0.20), 4.32 (± 0.16), and 1.58 (± 0.17) kcal mol^{-1}, respectively.

Effect of Salt on Binding—Free energies of binding of the wild-type and mutant peptides to the 0.5β Fv fragment were

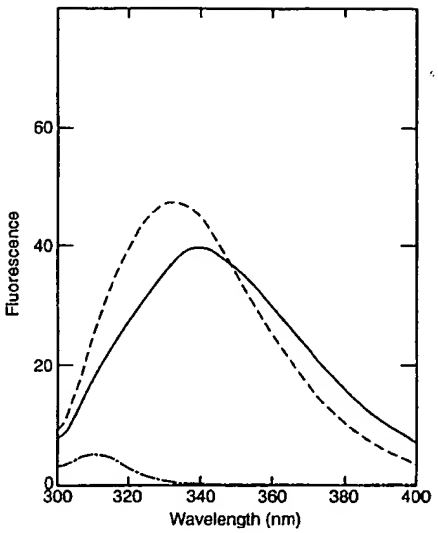

FIG. 2. **Fluorescence emission spectra of the 0.5β Fv fragment and its complex with the RP135 peptide antigen.** Fluorescence emission spectra of 300 nM 0.5β Fv fragment without (*continuous line*) and with (*broken line*) 1 μM RP135 peptide antigen were measured at 25.0 (± 0.1) °C in 50 mM phosphate buffer (pH 7.5) using an excitation wavelength of 280 nm with a band pass of 10 nm. Also shown is the spectrum of the buffer with and without peptide under the same conditions (*dashed line*).

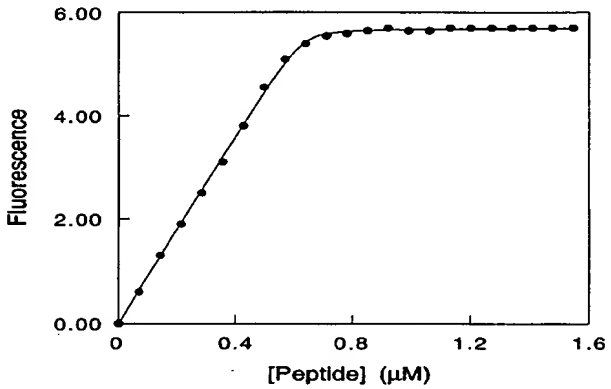

FIG. 3. **Titration of the 0.5β Fv fragment with wild-type peptide monitored by fluorescence enhancement.** The concentration of the 0.5β Fv fragment was 0.5 μM. The data were fitted to Equation 1. For further details, see "Experimental Procedures."

determined also in the presence of 1 M NaCl (Table I). The changes, upon addition of 1 M NaCl, in the free energies of binding of wild-type peptide and the R4A, R8A, and R11A mutants are 1.76 (± 0.17), 1.78 (± 0.13), 1.21 (± 0.03), and 0.79 (± 0.07) kcal mol^{-1}, respectively. In the presence of 1 M NaCl, the mutations R4A, R8A, and R11A reduce the binding energy to the 0.5β Fv fragment by 0.24 (± 0.09), 3.77 (± 0.08), and 0.61 (± 0.09) kcal mol^{-1}, respectively.

DISCUSSION

Amino acid sequence information had suggested that electrostatic interactions are of special importance in the binding of the RP135 peptide antigen to the 0.5β Fv antibody fragment. The 20-mer peptide contains 6 positively charged residues (4 arginines and 2 lysines) and no negatively charged residues whereas the antibody's complementarity determining regions contain many negatively charged residues and only a few positively charged residues. In addition, model building (5) showed that a shallow concave groove is formed by the 6 complementarity determining regions of the antibody and by two frame-

work residues (Tyr-49(H) and Trp-47(H)), and that this potential antigen-binding site contains many negatively charged side chains. Electrostatic interactions were previously demonstrated to be important in formation of other antibody-antigen complexes (24).

In order to determine the contribution of electrostatic interactions, we established a quantitative and highly accurate binding assay for the interaction of the RP135 peptide with the 0.5β Fv fragment. We then analyzed the effects of mutations of arginine residues in the peptide on its interaction with the 0.5β Fv fragment both in the absence and in the presence of 1 M NaCl (Table I). All arginine residues in the peptide were replaced except Arg-15 which was not, owing to its role in stabilizing the peptide conformation (7, 25). The free energies of binding of the wild-type and all of the mutant RP135 peptides to the 0.5β Fv fragment are found to decrease in the presence of 1 M NaCl demonstrating the importance of multiple electrostatic interactions in this system.

TABLE I

Free energies of binding of the 0.5β Fv fragment to wild-type and mutant RP135 peptides at 0 and 1 M NaCl

Each titration was carried out in duplicate (ΔG_1 and ΔG_2) at 25.0 °C as described under "Experimental Procedures." Free energies of binding were calculated from the dissociation constants, K, using: $\Delta G = RT\ln K$ where R is the gas constant and T is the absolute temperature.

Peptide	ΔG_1	ΔG_2	ΔG_{ave}[a]
		kcal mol^{-1}	
Wild-type (0 M salt)	−11.91 (±0.24)	−11.90 (±0.20)	−11.91 (±0.16)
R4A (0 M salt)	−11.76 (±0.15)	−11.62 (±0.19)	−11.69 (±0.12)
R8A (0 M salt)	−7.51 (±0.02)	−7.66 (±0.02)	−7.59 (±0.01)
R11A (0 M salt)	−10.39 (±0 08)	−10.27 (±0.07)	−10.33 (±0.05)
Wild-type (1 M salt)	−10.23 (±0.09)	−10.07 (±0.10)	−10.15 (±0.07)
R4A (1 M salt)	−9.95 (±0.09)	−9.87 (±0.07)	−9.91 (±0.06)
R8A (1 M salt)	−6.51 (±0.05)	−6.24 (±0.03)	−6.38 (±0.03)
R11A (1 M salt)	−9.40 (±0.06)	−9.67 (±0.08)	−9.54 (±0.05)

[a] $\Delta G_{ave} = 1/2(\Delta G_1 + \Delta G_2)$.

The mutations R8A and R11A, but not R4A, are found to have large effects on binding of the RP135 peptide to the 0.5β Fv fragment. Our precise measurements are in agreement with the more qualitative findings of Okada *et al.* (26) that mutation of the corresponding arginine residues in gp120 affect its binding to the 0.5β monoclonal antibody. Okada *et al.* (26) also showed that mutation of these arginine residues affects virus infectivity and syncytium-inducing ability. Our results are also consistent with a previous epitope mapping study by NMR (5) which showed that the antigenic determinant recognized by the Fab fragment of the 0.5β antibody consists of 16 residues (Lys-5 to Ile-20). Interestingly, in most HIV isolates there is a deletion in the V3 loop of two residues corresponding to Arg-8 and Gln-7 in RP135 (27) which may explain why the 0.5β antibody is strain-specific.

The salt-dependent components of the contributions to the binding energy of the arginine residues mutated in this study were isolated by invoking thermodynamic cycles shown in Fig. 4. By analogy to double-mutant cycles (28), the cycles in Fig. 4 consist of two different steps: (i) a mutation and (ii) transfer from 0 M NaCl to 1 M NaCl. The coupling free energies for such cycles are calculated using Equation 4, and they reflect to what extent the effect of the mutation is salt-dependent. If the coupling energy is zero, then the effect of the mutation is salt-independent. If the coupling energy is different from zero, then the effect of the mutation is salt-dependent. Surprisingly, it may be seen from Fig. 4 that there is no correlation between the magnitude of the salt-dependent contribution to the binding energy of a given residue and its apparent overall contribution.

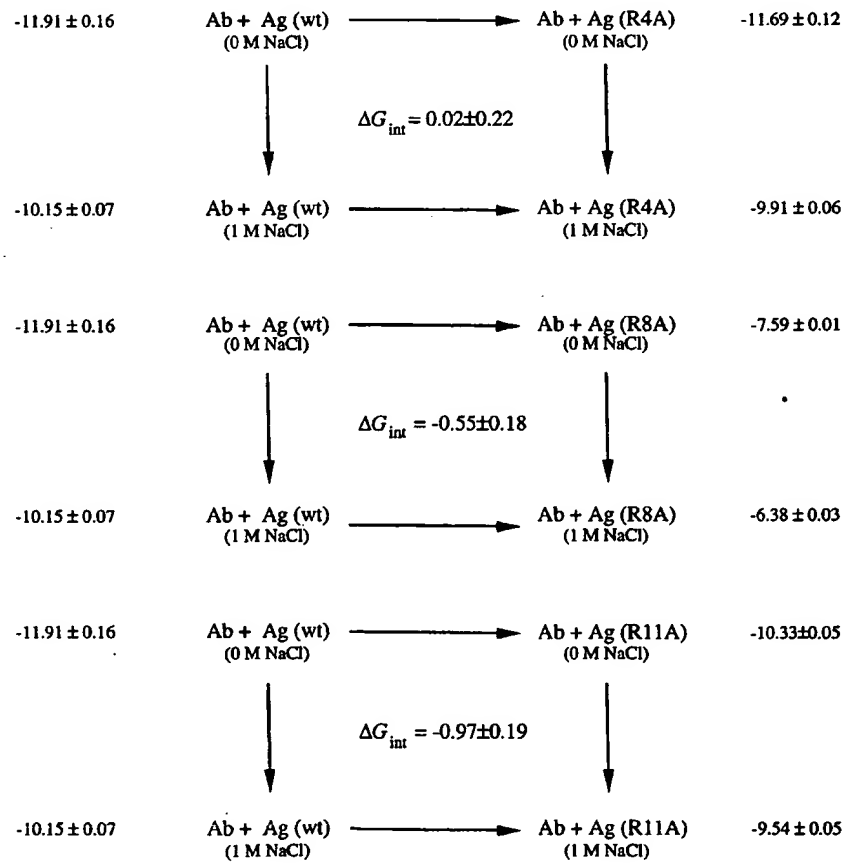

FIG. 4. **Thermodynamic cycles showing the coupling between effects of high salt and mutations in the peptide antigen on its binding to the 0.5β Fv fragment.** The Fv fragment and the wild-type peptide antigen are designated by *Ab* and *Ag(wt)*, respectively. Single-letter notation for amino acids is used. Free energy values are given in kcal mol^{-1} (Table I). The coupling free energies, ΔG_{int}, were calculated using Equation 4.

For example, the apparent contribution (ΔG_{app}) of Arg-8 to the binding energy is −4.32 (± 0 16) kcal mol^{-1} whereas the salt-dependent component of its contribution is only −0.55 (± 0.18) kcal mol^{-1}. In contrast, the apparent contribution of Arg-11 to the binding energy is −1.58 (± 0.17) kcal mol^{-1}, and the salt-dependent component of its contribution is −0.97 (± 0.19) kcal mol^{-1}. We can define ϕ as the ratio between the salt-dependent contribution, ΔG_{int}, and the apparent total contribution ($\phi = \Delta G_{int}/\Delta G_{app}$). The ϕ values for Arg-4, Arg-8, and Arg-11 are −0.09 (± 0.99), 0.13 (± 0.04), and 0.61 (± 0.14), respectively. There is uncertainty regarding the ϕ value for Arg-4 but it is clear that the salt-dependent contribution is more dominant in the case of Arg-11 compared with Arg-8. In principle, two reasons may account for this difference: (i) incomplete shielding by salt, *i.e.* Arg-11 is more solvent-exposed than Arg-8 in the Fv fragment-peptide complex or (ii) Arg-8 is involved in nonelectrostatic interactions. Further structural and energetic studies now in progress are required in order to distinguish between these possibilities.

The strength of exposed and buried salt bridges has been determined in other systems. In T4 lysozyme, a buried salt bridge was found to contribute 3–5 kcal mol^{-1} to protein stability (29) whereas solvent-exposed salt bridges in barnase were found to contribute only about 1 kcal mol^{-1} to its stability in the absence of high salt which had a strong masking effect on them (30). Here, both the magnitude of the mutational effect (ΔG_{app} = −4.32 (± 0.16) kcal mol^{-1}) and the extent of shielding by 1 M NaCl (ϕ = 0.13 (± 0.04)) suggest that Arg-8 is involved in a buried salt bridge. The magnitude of the mutational effect in the case of Arg-11 (ΔG_{app} = −1.58 (± 0.17) kcal mol^{-1}) and the extent of masking by salt (ϕ = 0.61 (± 0.14)) suggest that this residue is probably involved in a more solvent-exposed electrostatic interaction.

Acknowledgments—We thank Dr. S. Matsushita for the 54'CB1 hybridoma cell line producing the 0.5β monoclonal antibody. We also thank S. Rubinraut and Prof. M. Fridkin for peptide synthesis, Dr. M. Peretz and Prof. Y. Burstein for help with peptide purification, and Dr. S. Cabilly for advice at the early stages of this project.

REFERENCES

1. Matsushita, S., Robert-Guroff, M., Rusche, J., Koito, A., Hattori, T., Hoshino, H., Javaherian, K., Takatsuki, K., and Putney, S. (1988) *J. Virol.* **62**, 2107–2114
2. Emini, E. A., Schleif, W. A., Nunberg, J. H., Conley, A. J., Eda, Y., Tokiyoshi, S., Putney, S. D., Matsushita, S., Cobb, K. E., Jett, C. M., Eichberg, J. W., and Murthy, K. K. (1992) *Nature* **355**, 728–730
3. Goudsmit, J., Debouck, C., Meloen, R. H., Smit, L., Bakker, M., Asher, D. M., Wolff, A. V., Gibbs, C. J., Jr., and Gajdusek, D. C. (1988) *Proc. Natl. Acad. Sci. U. S. A.* **85**, 4478–4482
4. Palker, T. J., Clark, M. E., Langlois, A. J., Matthews, T. J., Weinhold, K. J., Randall, R. R., Bolognesi, D. P., and Haynes, B. F. (1988) *Proc. Natl. Acad. Sci. U. S. A.* **85**, 1932–1936
5. Zvi, A., Kustanovich, I., Feigelson, D., Levy, R., Eisenstein, M., Matsushita, S., Richalet- Sécordel, P., Regenmortel, M. H. V., and Anglister, J. (1995) *Eur. J. Biochem.* **229**, 178–187
6. Rini, J. M., Stanfield, R. L., Stura, E. A., Salinas, P. A., Profy, A. T., and Wilson, I. A. (1993) *Proc. Natl. Acad. Sci. U. S. A.* **90**, 6325–6329
7. Ghiara, J. B., Stura, E. A., Stanfield, R. L., Profy, A. T., and Wilson, I. A. (1994) *Science* **264**, 82–85
8. Winter, G., and Milstein, C. (1991) *Nature* **349**, 293–299
9. Skerra, A. (1993) *Curr. Opin. Immunol.* **5**, 256–262
10. Skerra, A., and Plückthun, A. (1988) *Science* **240**, 1038–1041
11. Riechmann, L., Foote, J., and Winter, G. (1988) *J. Mol. Biol.* **203**, 825–828
12. Huston, J. S., Levinson, D., Mudgett-Hunter, M., Tai, M.-S., Novotny, J., Margolies, M. N., Ridge, R. J., Bruccoleri, R. E., Haber, E., Crea, R., and Oppermann, H. (1988) *Proc. Natl. Acad. Sci. U. S. A.* **85**, 5879–5883
13. Bird, R. E., Hardman, K. D., Jacobson, J. W., Johnson, S., Kaufman, B. M., Lee, S.- M., Lee, T., Pope, S. H., Riordan, G. S., and Whitlow, M. (1988) *Science* **242**, 423–426
14. Better, M., Chang, C. P., Robinson, R. R., and Horwitz, A. H. (1988) *Science* **240**, 1041–1043
15. Reichmann, L., Cavanagh, J., and McManus, S. (1991) *FEBS Letters* **287**, 185–188
16. Marasco, W. A., Haseltine, W. A., and Chen, S. (1993) *Proc. Natl. Acad Sci. U. S. A.* **90**, 7889–7893
17. Matsushita, S., Maeda, H., Kimachi, K., Eda, Y., Maeda, Y., Murakami, T., Tokiyoshi, S., and Takatsuki, K. (1992) *AIDS Res. Hum. Retroviruses* **8**, 1107–1115
18. Orlandi, R., Güssow, D. H., Jones, P. T., and Winter, G. (1989) *Proc. Natl. Acad. Sci. U. S. A.* **86**, 3833–3837
19. Mead, D. A., Szczesna-Skopura, E., and Kemper, B. (1986) *Prot. Eng.* **1**, 67–74
20. Sayers, J. R., Schmidt, W., and Eckstein, F. (1988) *Nucleic Acids Res.* **16**, 791–802
21. Gill, S. C., and von Hippel, P. H. (1989) *Anal. Biochem.* **182**, 319–326
22. Snyder, S. L., and Sobocinski, P. Z. (1975) *Anal. Biochem.* **64**, 284–288
23. Skinner, M. A., Ting, R., Langlois, A. J., Weinhold, K. J., Lyerly, H. K., Javaherian, K., and Matthews, T. J. (1988) *AIDS Res. Human Retroviruses* **4**, 187–197
24. Novotny, J., and Sharp, K. (1992) *Prog. Biophys. Mol. Biol.* **58**, 203–224
25. Zvi, A., Hiller, R., and Anglister, J. (1992) *Biochemistry* **31**, 6972–6979
26. Okada, T., Patterson, B. K., Otto, P. A., and Gurney, M. E. (1994) *AIDS Res. Human Retroviruses* **10**, 803–811
27. LaRosa, G. J., Davide, J. P., Weinhold, K., Waterbury, J. A., Profy, A. T., Lewis, J. A., Langlois, A. J., Dreesman, G. R., Boswell, R. N., Shadduck, P., Holley, L. H., Karplus, M., Bolognesi, D. P., Matthews, T. J., Emini, E. A., and Putney, S. D. (1990) *Science* **249**, 932–935
28. Horovitz, A., and Fersht, A. R. (1990) *J. Mol. Biol.* **214**, 613–617
29. Anderson, D. E., Becktel, W. J., and Dahlquist, F. W. (1990) *Biochemistry* **29**, 2403–2408
30. Horovitz, A., Serrano, L., Avron, B., Bycroft, M., and Fersht, A. R. (1990) *J. Mol. Biol.* **216**, 1031–1044
31. Laemmli, U. K. (1970) *Nature* **227**, 680–685